Rassegna delle evidenze sperimentali sul $g-2$ del muone

Alberto Lusiani, per la collaborazione FNAL Muon g-2

Scuola Normale Superiore and INFN, sezione di Pisa

SCUOLA NORMALE SUPERIORE

INFN PISA

Giornata di approfondimento sul problema di g-2

Laboratori Nazionali del Gran Sasso

9 settembre 2021

INFN LNGS

Magnetic momentum

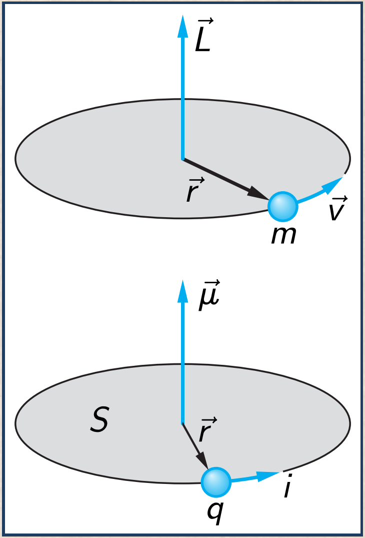

- $i = \frac{q}{T} = q\frac{v}{2\pi r}$
- $\mu = iS = q\frac{v}{2\pi r}\pi r^2 = \frac{q}{2}r\frac{mv}{m} = \frac{q}{2m}L$
- $\vec{\mu} = \frac{q}{2m}\vec{L}$

precession of magnetic momentum in magnetic field

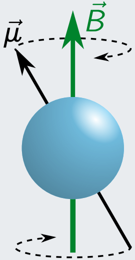

Standard model of particle physics

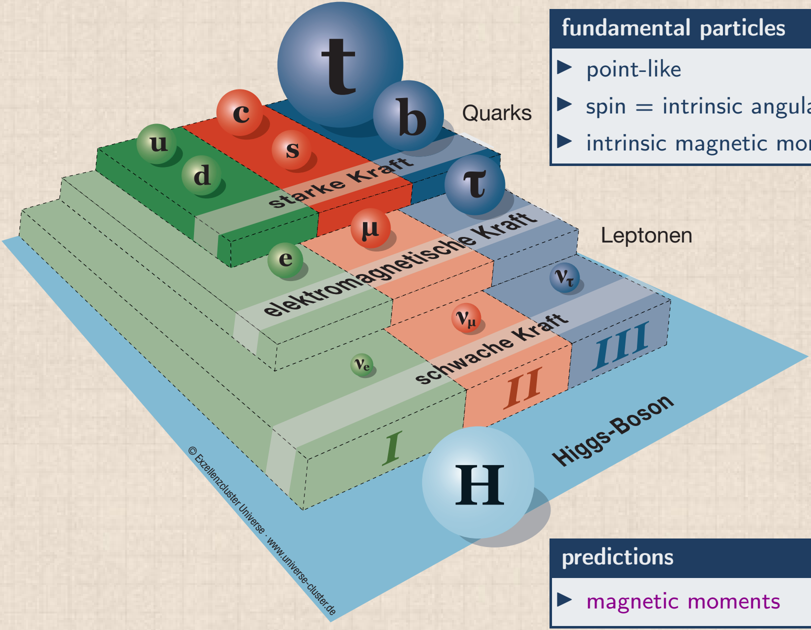

fundamental particles

- point-like
- spin = intrinsic angular momentum
- intrinsic magnetic momentum

model parameters

- masses (Higgs couplings)
- spins
- charges
- coupling constants

predictions

- magnetic moments

Some notation

particle x such as a muon, electron, proton, neutron

- magnetic moment $\vec{\mu}_x = g_x \dfrac{e}{2m_x} \vec{S}_x$,
  - $e =$ absolute value of electron charge (used also for neutron)
  - $\vec{S}_x =$ spin (particle intrinsic angular momentum)
  - $g_x =$ gyromagnetic ratio (defined also for neutral particles)
- classical charge distribution: $\rho_q/\rho_m =$ constant $\Rightarrow$ $g = 1$

leptons (electron, muon, tau): spin 1/2 fundamental point-like particles

- $g_e,\ g_\mu,\ g_\tau = 2$ at first order and for Dirac equation (note: negative sign omitted for simplicity)
- $g_e,\ g_\mu,\ g_\tau > 2$ including effects of virtual particles exchanges
- $a_x = \dfrac{g_x - 2}{2}$ anomalous gyromagnetic ratio or magnetic anomaly
- Standard Model precisely predicts g_x, a_x

proton, neutron

- $g_p \simeq 5.6$, $g_n \simeq -3.8$
- composite particles made of three quarks (mainly interacting with strong force)
- no precise Standard Model prediction of their magnetic moments
- strong force interactions are non-perturbative at low energy and difficult to compute

Wisdom On Difficult Experiments

"If you enjoy doing difficult experiments, you can do them, but it is a waste of time and effort because the result is already known" : Pauli

"No experiment is so dumb, that it should not be tried" : Gerlach

First g_μ measurement (1957)

motivation: confirm Lee & Yang predictions about parity violation in pion and muon decay

Observations of the Failure of Conservation of Parity and Charge Conjugation in Meson Decays: the Magnetic Moment of the Free Muon*

Richard L. Garwin,† Leon M. Lederman, and Marcel Weinrich

Physics Department, Nevis Cyclotron Laboratories, Columbia University, Irvington-on-Hudson, New York

(Received January 15, 1957)

LEE and Yang[1–3] have proposed that the long held space-time principles of invariance under charge conjugation, time reversal, and space reflection (parity) are violated by the "weak" interactions responsible for decay of nuclei, mesons, and strange particles. Their hypothesis, born out of the $\tau - \theta$ puzzle,[4] was accompanied by the suggestion that confirmation should be sought (among other places) in the study of the successive reactions

$$\pi^+ \to \mu^+ + \nu, \quad (1)$$

$$\mu^+ \to e^+ + 2\nu. \quad (2)$$

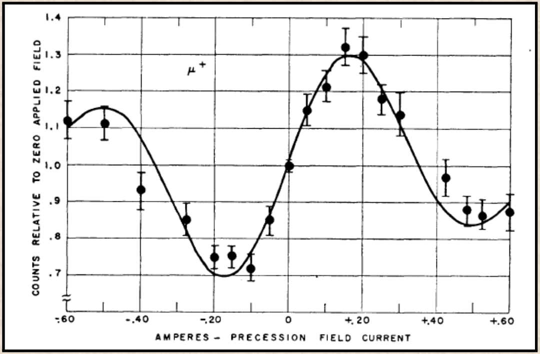

- forward pion-decay muons are highly polarized
- μ-decay electrons angular asymmetry vs. μ spin
- electron rate vs. B field applied to muons
- $g_\mu = 2.01 \pm 0.01$

Measurement Principle

Experiments with a Polarized Muon Beam

By J. M. CASSELS, T. W. O'KEEFFE, M. RIGBY, A. M. WETHERELL and J. R. WORMALD
Nuclear Physics Research Laboratory, University of Liverpool

MS. received 2nd April 1957

Columbia, Liverpool, CERN

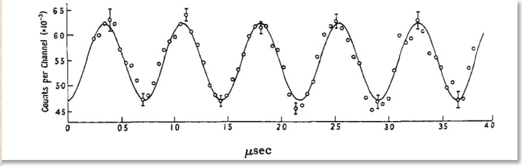

g = 2.004 +- 0.014

First sub % measurement of g

It may be remarked that a much more accurate value of g/m_μ will surely be obtained by a resonance flip type of experiment, but the value of g itself should be sought in a comparison of the precession $(geH/2m_\mu c)$ and cyclotron $(eH/m_\mu c)$ frequencies of muons in a magnetic field. The two frequencies are expected to differ only by the radiative correction.

a_μ measurements and predictions 1979 – March 2021 (incomplete collection)

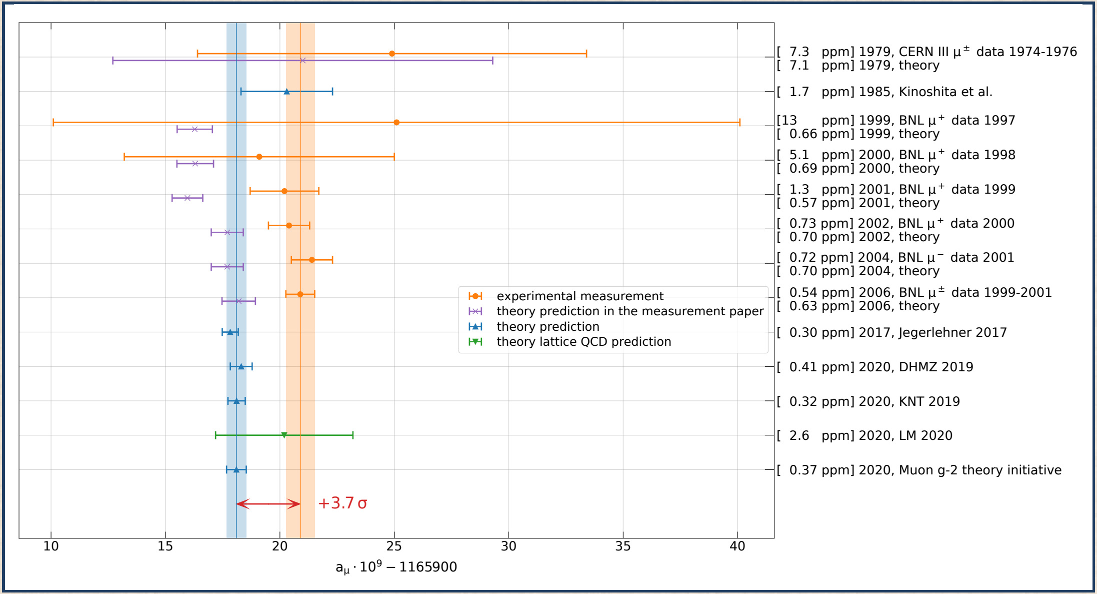

a_μ measurements and predictions 1979 – March 2021 (incomplete collection)

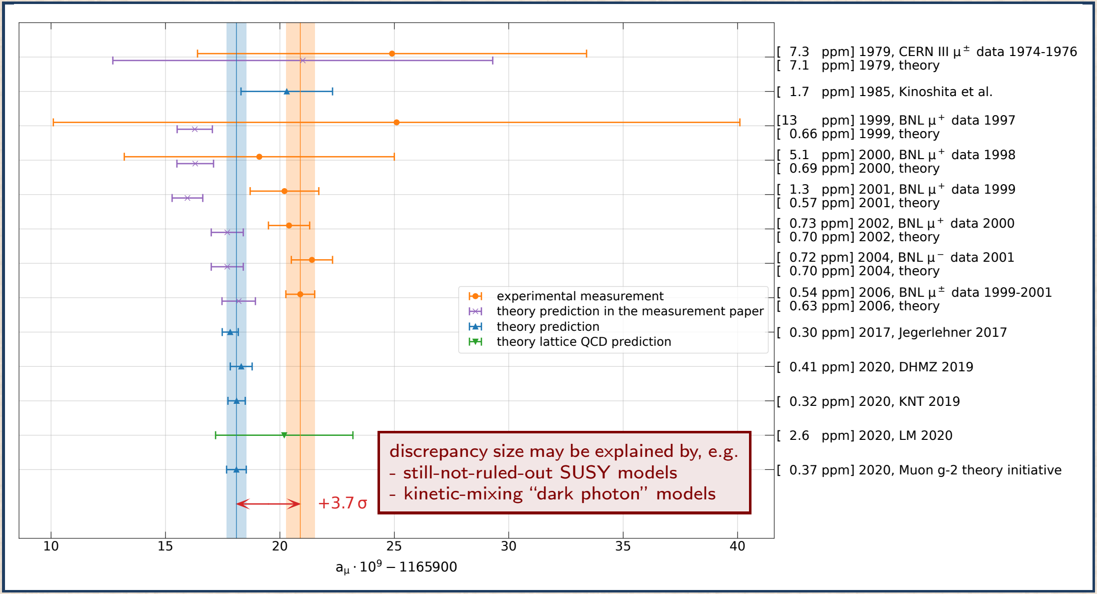

Motion and spin precession of muon in uniform magnetic field

muon spin precession relative to momentum

$$\omega_s \quad - \quad \omega_c \quad = \quad \omega_a$$

$$-g_\mu \frac{eB}{2m_\mu} - (1-\gamma)\frac{eB}{m_\mu \gamma} - \left(-\frac{eB}{m_\mu \gamma} \right) = -a_\mu \frac{eB}{m_\mu}$$

Larmor + Thomas precessions — cyclotron frequency — no γ!

- frequency measurements best for precision
- magnetic field NMR measurement also frequency
- angle between momentum and spin $\theta(t) = \omega_a t$

polarized muons in magnetic storage ring

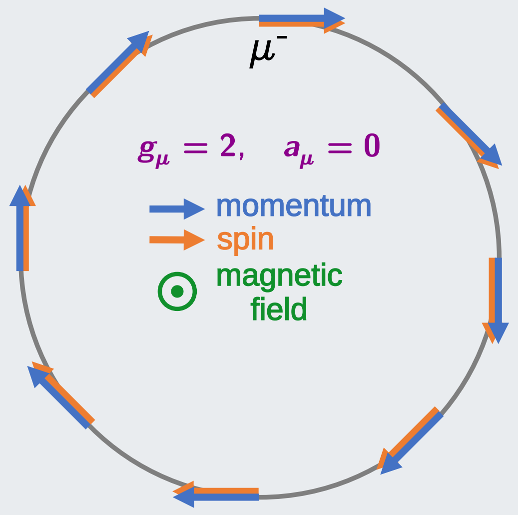

Motion and spin precession of muon in uniform magnetic field

muon spin precession relative to momentum

$$\omega_s \quad - \quad \omega_c \quad = \quad \omega_a$$

$$-g_\mu \frac{eB}{2m_\mu} - (1-\gamma)\frac{eB}{m_\mu\gamma} - \left(-\frac{eB}{m_\mu\gamma}\right) = -a_\mu \frac{eB}{m_\mu}$$

Larmor + Thomas precessions — cyclotron frequency — no γ!

- frequency measurements best for precision
- magnetic field NMR measurement also frequency
- angle between momentum and spin $\theta(t) = \omega_a t$

polarized muons in magnetic storage ring

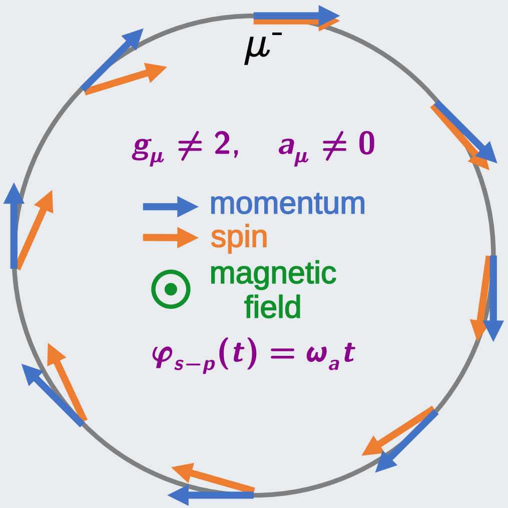

Focusing electric field and magic energy

in presence of (focusing) electric field and motion not perfectly transverse to magnetic field

$$\vec{\omega}_a = -\frac{e}{m_\mu}\left[a_\mu \vec{B} - \left(a_\mu - \frac{1}{\gamma^2-1}\right)(\vec{\beta}\times\vec{E}) - a_\mu \frac{\gamma}{\gamma+1}\left(\vec{\beta}\cdot\vec{B}\right)\vec{\beta}\right]$$

CERN 1975-, BNL, FNAL

$$p_\mu^{\text{magic}} = 3.094\,\text{GeV} \quad\Rightarrow\quad \gamma = 29.3$$

$$\Rightarrow \quad \left(a_\mu - \frac{1}{\gamma^2-1}\right) \simeq 0$$

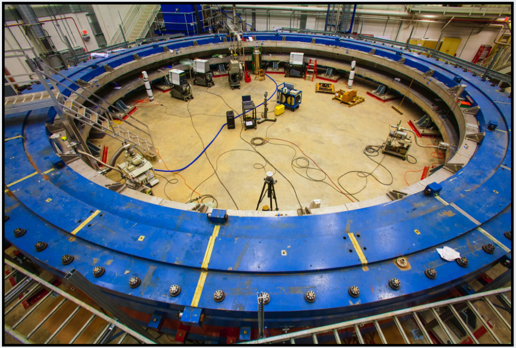

J-PARC E34

ultra-cold muons

$$E = 0 \quad\Rightarrow\quad \vec{\beta}\times\vec{E} = 0$$

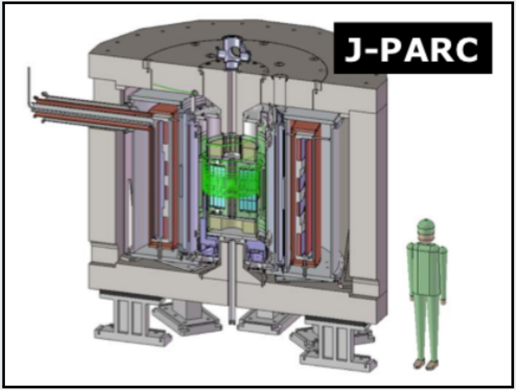

Rate of high-energy muon-decay electrons modulated with $\cos \omega_a t$

- because of parity violation in muon decay, decay electrons peak along muon spin

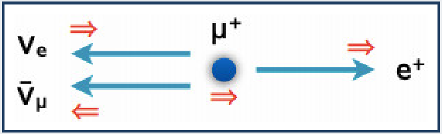

- electrons decaying along muon momentum have highest energy in laboratory frame
- $N_e(E_e > E_t) = N_{e0} e^{-t/\tau_\mu} (1 + A \cos \omega_a t)$

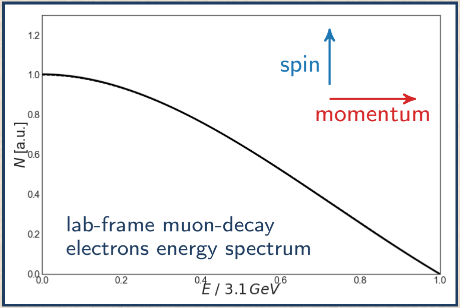

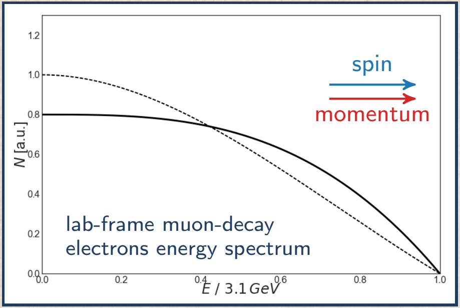

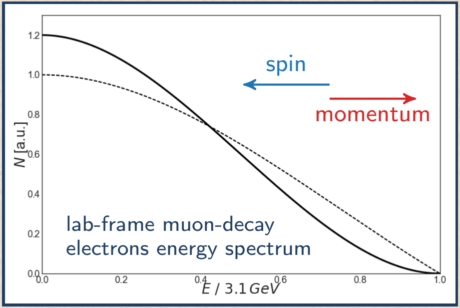

Production of polarized muons

- dump 8 GeV protons on target to produce pions
- select pions with momemtum $p \simeq 3.11$ GeV
- let them decay into muons
- in pion rest frame, because of parity violation in pion decay, μ^- spin is aligned with momentum (μ^+ spin is anti-aligned with momentum)
- in laboratory frame, highest energy muons are >90% polarized

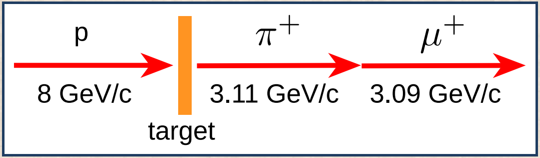

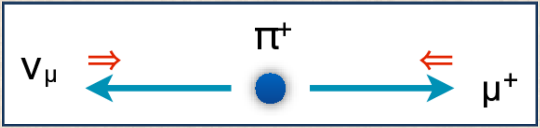

- with 8 GeV protons on target, μ^+ are produced $\sim 4\times$ more frequently than μ^-

a_μ measurement: how sub-ppm precision can be obtained

measurement of magnetic field: ω_p

- proton spin precession frequency measures magnetic field (NMR): $\hbar\omega_p = 2\mu_p B$

measurements

- $\omega_a = a_\mu \frac{eB}{m_\mu}, \quad \hbar\omega_p = 2\mu_p B$

spin 1/2 particle x = proton, muon

- $S_x = \frac{\hbar}{2}, \quad \mu_x = g_x \frac{e}{m_x} S, \quad a_x = \frac{g_x - 2}{2}$

$$a_\mu = \frac{\omega_a/\omega_p}{\mu_\mu/\mu_p - \omega_a/\omega_p}$$

muonium & hydrogen hyperfine transitions

mainly LAMPF 1999 experiment
precision on CODATA 2018 fit: 22 ppb

actually, best a_μ obtained by adding ω_a/ω_p measurement to Fundamental Physical Constants CODATA fit

ω_a & ω_p in same magnetic field

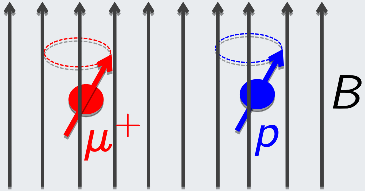

Measurement formula in more detail

$$a_\mu = \left[\frac{\omega_a}{\tilde{\omega}'_p(T)}\right] \cdot \left[\frac{\mu'_p(T)}{\mu_e(\mathrm{H})}\right] \left[\frac{\mu_e(H)}{\mu_e}\right] \left[\frac{m_\mu}{m_e}\right] \left[\frac{g_e}{2}\right]$$

(equivalent to $a_\mu = \dfrac{\omega_a/\omega_p}{\mu_\mu/\mu_p - \omega_a/\omega_p}$ using CODATA constants)

measurements by the Muon $g-2$ collaboration

- ω_a — precession of muon spin relative to momentum rotation in magnetic field
- $\tilde{\omega}'_p(T)$ — precession frequency of shielded proton spin in spherical water sample at $T = 34.7\,^\circ\mathrm{C}$ in muon-beam-weighted magnetic field, $\tilde{\omega}'_p(T) = \langle \omega'_p(T)(x,y,\varphi) \times M(x,y,\varphi)\rangle$

notation

- $\mu'_p(T)$ — magnetic momentum of proton in spherical water sample at $34.7\,^\circ\mathrm{C}$
- $\mu_e(\mathrm{H})$ — magnetic momentum of electron in hydrogen atom

external measurements

- $\mu'_p(T)/\mu_e(H)$ — 10.5 ppb precision, Metrologia 13, 179 (1977)
- $\mu_e(H)/\mu_e$ — 5 ppq (negligible) theory QED calculation, Rev. Mod. Phys. 88 035009 (2016)
- m_μ/m_e — 22 ppb precision — CODATA 2018 fit, primarily driven by LAMPF 1999 measurements of muonium hyperfine splitting, Phys. Rev. Lett. 82, 711 (1999)
- $g_e/2$ — 0.28 ppt (negligible), Phys. Rev. Lett. 100, 120801 (2008)

a_μ experimental precision

FNAL-E989 design precision, compared to BNL-E821 final report (2006)

	BNL E821 (2006)	FNAL E989 final goal	
ω_a statistical	460 ppb	100 ppb	$\times 21$ detected muon decays ($1.6 \cdot 10^{11}$)
ω_a systematic	210 ppb	70 ppb	faster calorimeter with laser calibration, tracker
ω_p systematic	170 ppb	70 ppb	more uniform B, improve NMR measurement
external measurements	negligible	negligible	
total	540 ppb	140 ppb	

FNAL Muon $g-2$ collaboration

USA
- Boston
- Cornell
- Illinois
- James Madison
- Kentucky
- Massachusetts
- Michigan
- Michigan State
- Mississippi
- North Central
- Northern Illinois
- Regis
- Virginia
- Washington

USA National Labs
- Argonne
- Brookhaven
- Fermilab

China
- Shanghai Jiao Tong

Germany
- Dresden
- Mainz

Italy
- Frascati
- Molise
- Naples
- Pisa
- Roma Tor Vergata
- Trieste
- Udine

Korea
- CAPP/IBS
- KAIST

Russia
- Budker/Novosibirsk
- JINR Dubna

United Kingdom
- Lancaster/Cockcroft
- Liverpool
- Manchester
- University College London

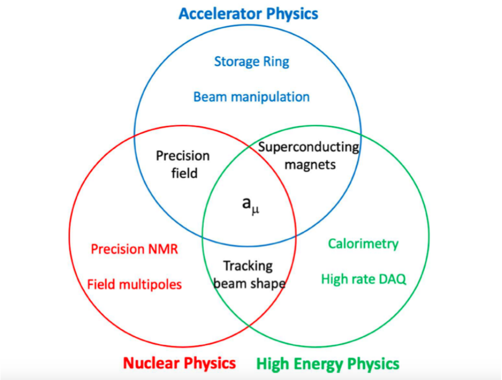

~200 collaborators
~40 institutions
7 countries

FNAL Muon $g-2$ collaborators, Elba Island, Spring 2019

BNL storage ring magnet moved to FNAL in 2013 (35 days long trip)

Storage ring magnet adjusted for maximum uniformity

wedging and shimming

- magnet adjusted to obtain 50 ppm field uniformity
- 3× better than at BNL

adjustements and insertions

- 72 poles
- 864 wedges
- 24 iron top hats
- 8000 surface iron foils

magnetic field made uniform to 50 ppm

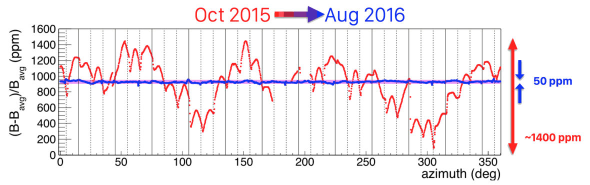

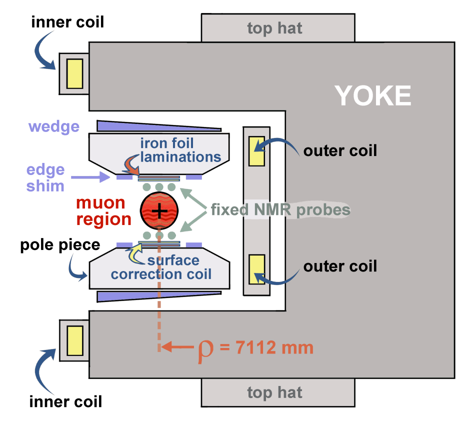

Muon production, storage and decay at FNAL

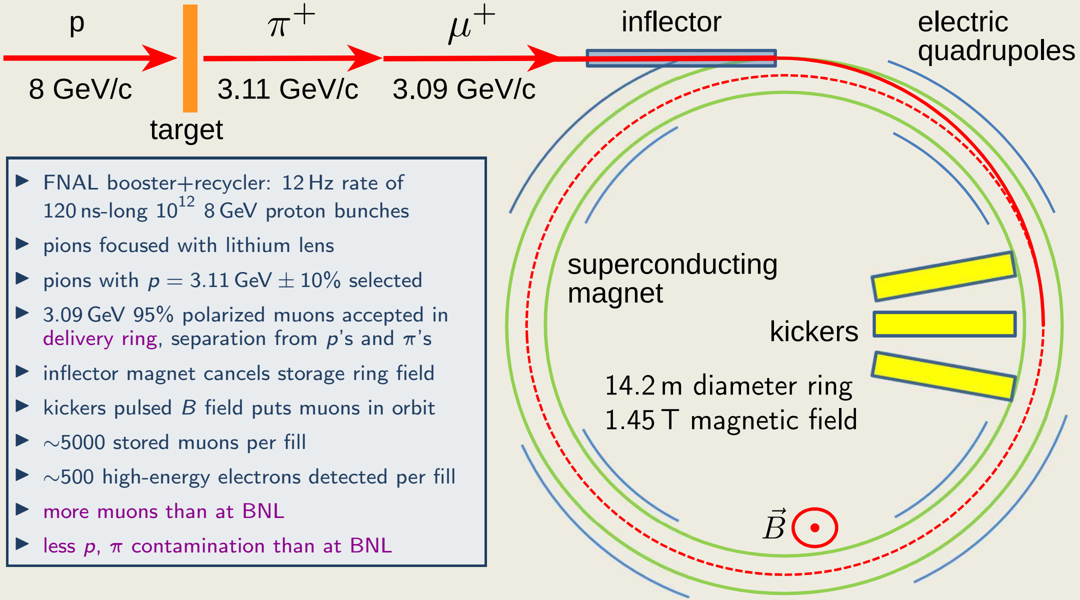

- FNAL booster+recycler: 12 Hz rate of 120 ns-long 10^{12} 8 GeV proton bunches
- pions focused with lithium lens
- pions with $p = 3.11$ GeV $\pm$ 10% selected
- 3.09 GeV 95% polarized muons accepted in delivery ring, separation from p's and π's
- inflector magnet cancels storage ring field
- kickers pulsed B field puts muons in orbit
- $\sim$5000 stored muons per fill
- $\sim$500 high-energy electrons detected per fill
- more muons than at BNL
- less p, π contamination than at BNL

Muon production, storage, decay and detection at FNAL

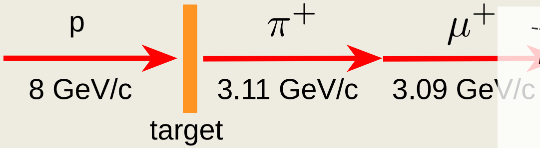

Muon decays detectors

- 24 calorimeters
- 2 trackers

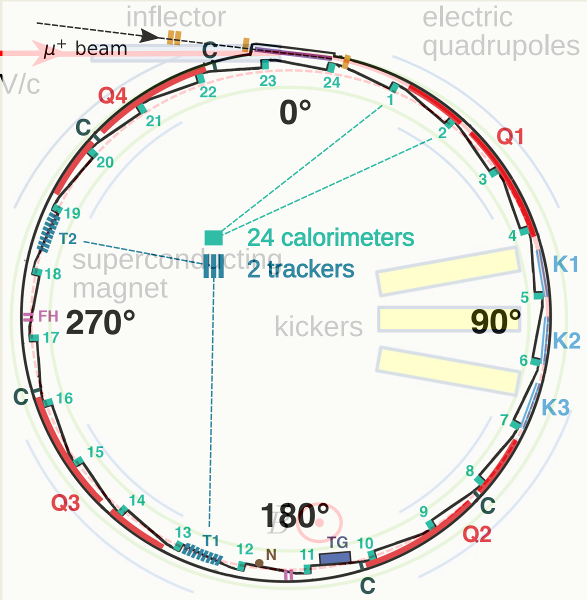

FNAL-E989 storage ring and detectors

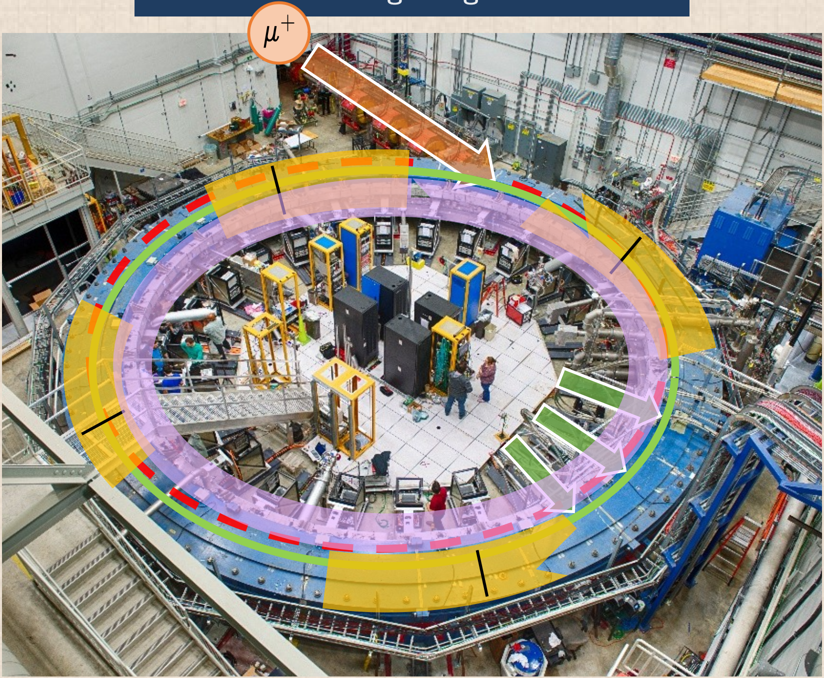

Muon decays detectors

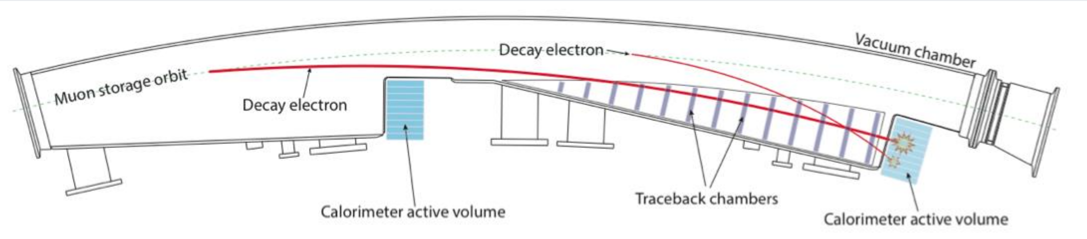

- 24 calorimeter modules of 6×9 PbF_2 crystals with 800 MHz-sampling SiPM readout
  - measure muon-decay electrons energy detecting Cherenkov light
  - accurate gain monitoring with laser calibration system
- 2 straw chamber trackers with total of about 1000 channels
  - reconstruct beam distribution inside storage ring from muon decay electrons

comparison with E821

- more granular calorimeter, faster data acquisition
- improved calorimeter gain monitoring
- improved tracking

Conceptual formula for $R'_\mu(T) = \omega_a/\tilde{\omega}'_p(T)$

$$R'_\mu(T) = \frac{\omega_a}{\tilde{\omega}'_p(T)} \overset{\text{conceptually}}{=} \frac{f_{\text{blind}}\ \omega_a^{\text{m}}\ \left(1 + C_e + C_p + C_{\text{ml}} + C_{\text{pa}}\right)}{f_{\text{calib}}\ \langle \omega'_p(T)(x,y,\varphi) \times M(x,y,\varphi)\rangle\ (1 + B_k + B_q)}$$

ω_a measurement and corrections

- f_{blind} correction for blinding clock offset
- ω_a^m *measured* precession of muon spin relative to momentum rotation in magnetic field
- C_e ω_a electric field correction
- C_p ω_a pitch correction (vertical beam oscillations)
- C_{ml} ω_a muon loss correction
- C_{pa} ω_a phase acceptance correction

$\tilde{\omega}'_p(T)$ measurement and corrections

- f_{calib} magnetic field probes calibration
- $\omega'_p(T)(x,y,\varphi)$ measured shielded proton spin precession frequency map in storage ring
- $M(x,y,\varphi)$ muon beam distribution
- B_k $\tilde{\omega}'_p(T)$ kicker eddy fields correction
- B_q $\tilde{\omega}'_p(T)$ electric quadrupoles transient field correction

Multiple analysis groups

ω_a^m

- 11 different measurements
- by 6 analysis groups
- using 4 different methods to fit rate of muon-decay positrons over time

$\tilde{\omega}'_p(T)$

- 2 different measurements
- by 2 analysis groups
- using 2 different methods

Run 1 data samples, collected in 2018

muon decays

Dataset	# Days (Apr-Jun 2018)	Tune (n)	Kicker (kV)	# fills [10^4]	# positrons [10^9]
1a	3	0.108	130	151	0.92
1b	7	0.120	137	196	1.28
1c	9	0.120	132	333	1.98
1d	24	0.107	125	733	4.00

total of 8.2 billion positrons ($\sim$1.2$\times$ BNL), $\sim$6% of E989 goal of 21$\times$ BNL
4 run periods with different kickers and quadrupoles settings, hence different beam dynamics

magnetic field

magnetic field measurements weighted by detected muon decays

Blinding procedures (f_{blind})

- 40 MHz base nominal clock used for ω_a data acquisition modified with random ±25 ppm offset
- secret offset conserved by two persons that are not members of the collaboration
- each year of data-taking (Run) is separately blinded
- second software blinding offset for each of the independent ω_a analysis groups (honor-code based)

blinding of 2018 Run

blinded clock for 2018

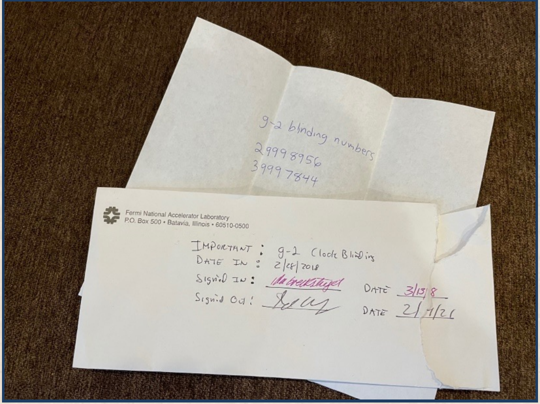

Reconstruction of positron energy deposits in calorimeters

readout

- record SiPM samples for all deposits $> 50\,\text{MeV}$

fit using crystal pulses templates

- get template pulse for each crystal from data
- samples fit to one or more superposed templates

two reconstruction algorithms

- local: fit individual crystals
- global: global fit over multiple crystals

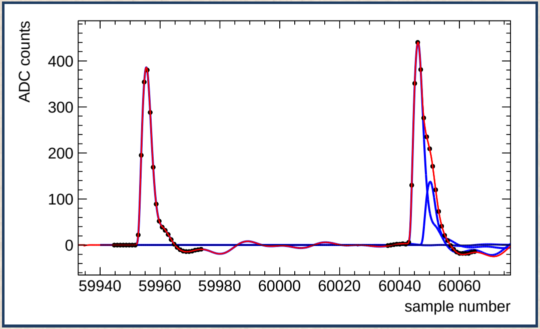

Calorimeter gain variation, measured with laser pulses and corrected

- SiPM gain is reduced by occurrence of preceding hits
- gain monitored by reading back reference laser light pulses injected in PbF_2 crystals
- positron energy measurement from SiPM readout corrected for average measured gain loss

μs time scale SiPM power supply recovery time

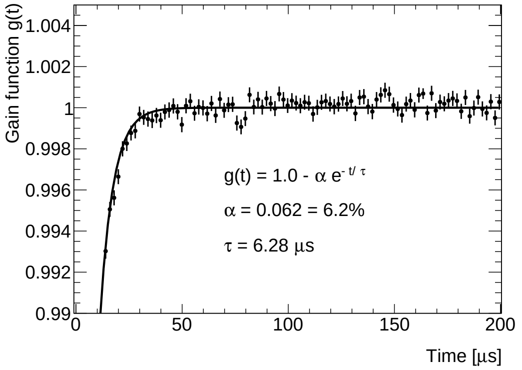

ns time scale SiPM pixel recovery time

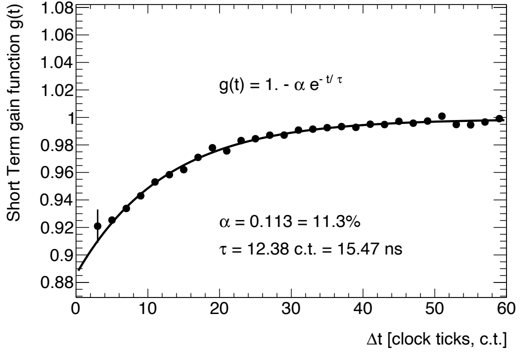

Laser-based gain monitoring built and operated by Italian collaborators

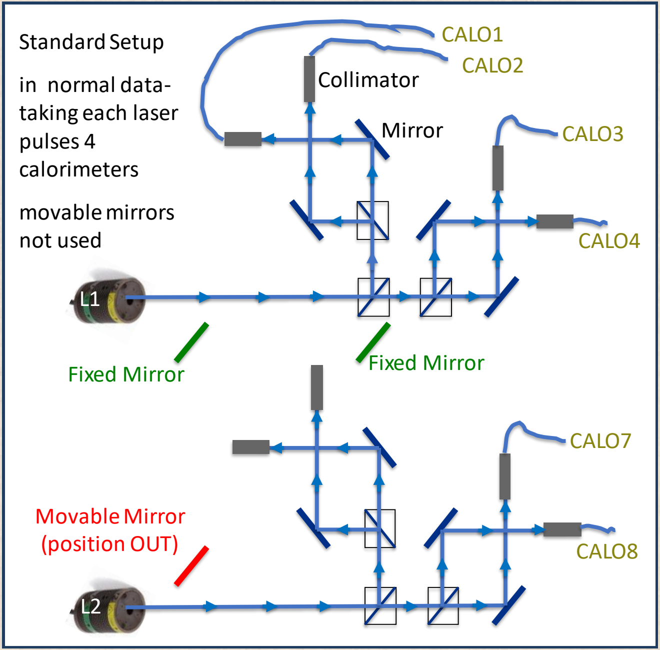

Laser-based gain monitoring built and operated by Italian collaborators

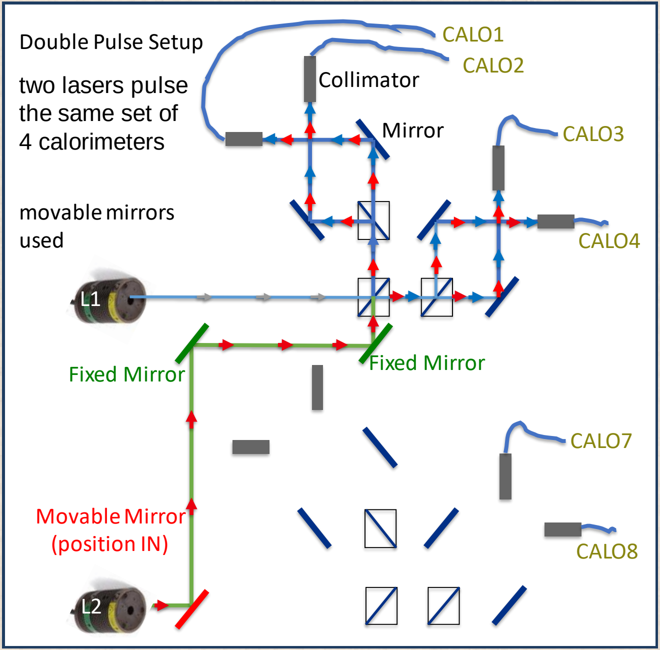

Pileup, statistically subtracted

3 methods of pileup estimation

- combine hit with 2nd hit in shadow window
  - (1) sum 2 hits using model to get E, t
  - (2) reconstruct pileup hit using all crystals ADC counts
- (3) convolve hit density $\rho(E,t)$, then use estimated pileup and iteratively solve for the pileup-subtracted $\rho'(E,t)$

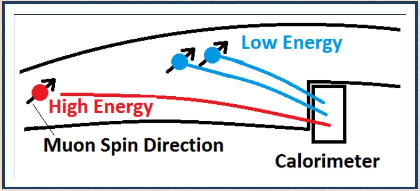

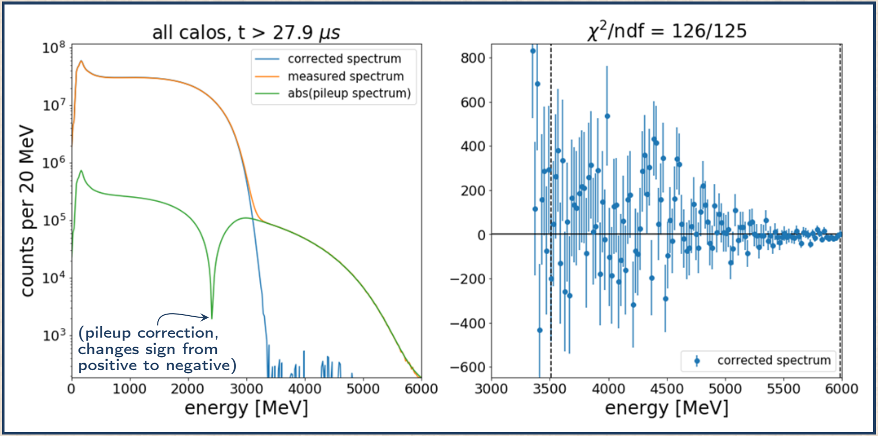

Muon $g-2$ wiggle plot

number of detected positrons with $E > E_t$ in bins of time

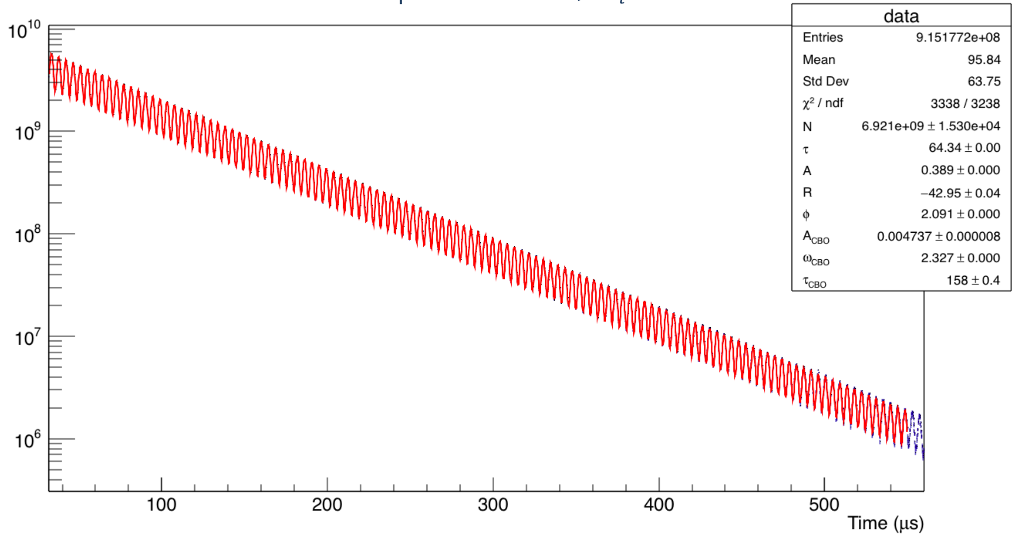

Muon precession, 5 parameters ω_a fit model

- number of positron decays with $E > \sim 1.7$ GeV, binned over time, from 30 to 650 μs
- fit with $N(t) = N_0 e^{-t/\tau_\mu} [1 + A\cos(\omega_a t + \varphi)]$

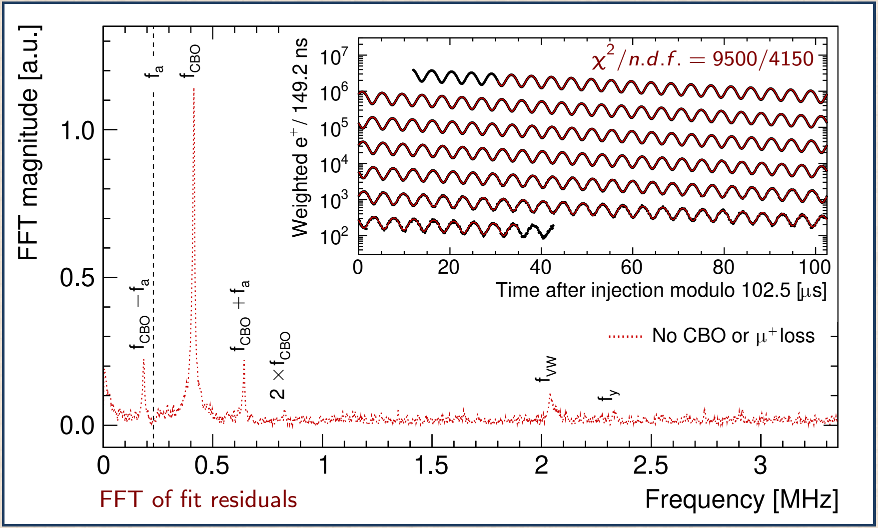

Extend ω_a fit model to account for lost muons on collimators

- some muons hit collimators and are lost
- muon loss rate during a fill measured with 3-4-5 coincidences of m.i.p. on calorimeters
- overall normalization of muon loss included as fit parameter

muon loss vs. time

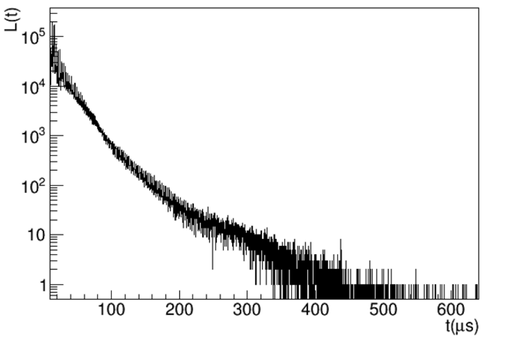

energy in calorimeter vs. momentum in tracker

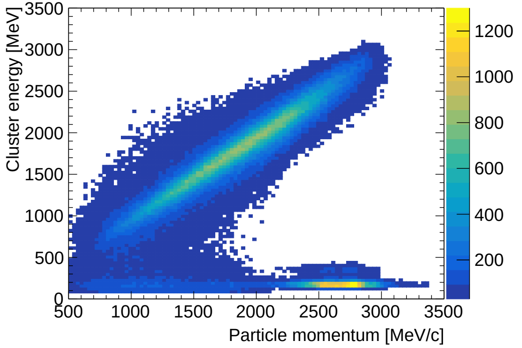

Muon precession, 22-parameters ω_a fit

- include beam dynamics oscillations of beam position and spread
- include effect of muon loss on collimators

$$N_0\, e^{-\frac{t}{\gamma\tau}}\, (1 + A \cdot A_{BO}(t) \cos(\omega_a t + \varphi + \varphi_{BO}(t))) \cdot N_{\text{CBO}}(t) \cdot N_{\text{VW}}(t) \cdot N_y(t) \cdot N_{\text{2CBO}}(t) \cdot \Lambda(t)$$

$$A_{\text{BO}}(t) = 1 + A_A \cos(\omega_{\text{CBO}}(t) \cdot t + \varphi_A) e^{-\frac{t}{\tau_{\text{CBO}}}}$$

$$\varphi_{\text{BO}}(t) = A_\varphi \cos(\omega_{\text{CBO}}(t) \cdot t + \varphi_\varphi) e^{-\frac{t}{\tau_{\text{CBO}}}}$$

$$N_{\text{CBO}}(t) = 1 + A_{\text{CBO}} \cos(\omega_{\text{CBO}}(t) \cdot t + \varphi_{\text{CBO}}) e^{-\frac{t}{\tau_{\text{CBO}}}}$$

$$N_{\text{2CBO}}(t) = 1 + A_{\text{2CBO}} \cos(2\omega_{\text{CBO}}(t) \cdot t + \varphi_{\text{2CBO}}) e^{-\frac{t}{2\tau_{\text{CBO}}}}$$

$$N_{\text{VW}}(t) = 1 + A_{\text{VW}} \cos(\omega_{\text{VW}}(t) \cdot t + \varphi_{\text{VW}}) e^{-\frac{t}{\tau_{\text{VW}}}}$$

$$N_y(t) = 1 + A_y \cos(\omega_y(t) \cdot t + \varphi_y) e^{-\frac{t}{\tau_y}}$$

$$\Lambda(t) = 1 - k_{LM} \int_{t_0}^{t} L(t') e^{t'/\tau} dt'$$

$$\omega_{\text{CBO}}(t) = \omega_0^{CBO} + \frac{A}{t} e^{-\frac{t}{\tau_A}} + \frac{B}{t} e^{-\frac{t}{\tau_B}}$$

$$\omega_y(t) = F \omega_{\text{CBO}}(t) \sqrt{2\omega_c / F \omega_{\text{CBO}}(t) - 1}$$

$$\omega_{\text{VW}}(t) = \omega_c - 2\omega_y(t)$$

22 parameters ω_a fit has χ^2/n.d.o.f. consistent with 1

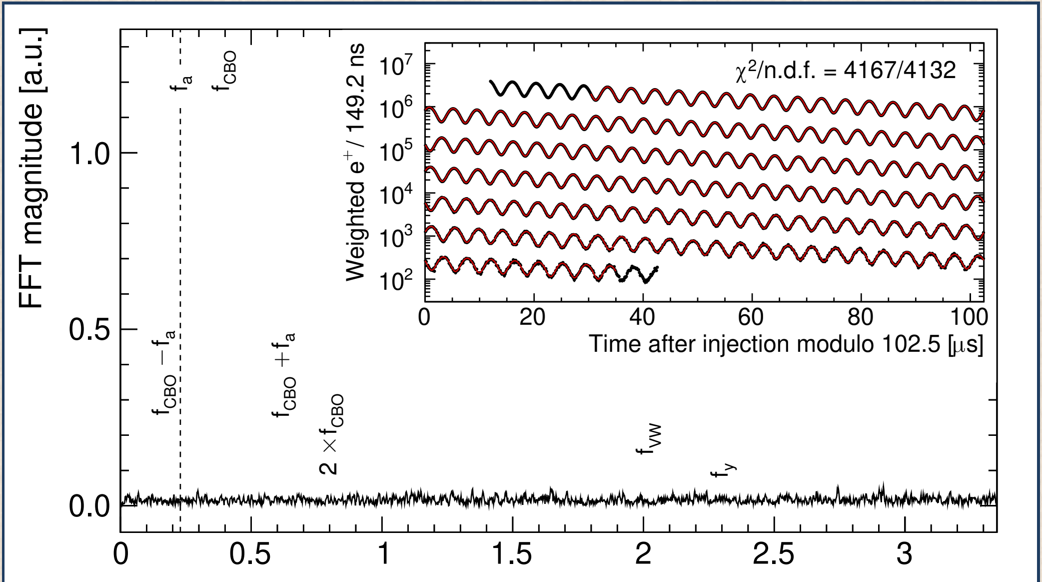

FFT of fit residuals

6 analysis groups, 4 analysis methods, 11 ω_a fits

4 analysis methods

- T (threshold): $\sum N(E_{e^+})$ — $E_{e^+} > 1.7$ GeV
- R (ratio): (see below) — $E_{e^+} > 1.7$ GeV
- A (asymmetry): $\sum A \cdot N(E_{e^+})$ — $E_{e^+} > 1.0$ GeV
- Q (charge): $\sum$ energy deposits — no threshold

ratio method

- randomly split time-binned positron decays in 4 sets
- displace time of two sets by $\pm T_a/2$
- ratio of 2 linear combinations can be fitted with just $A\cos(\omega_a t + \varphi)$ (instead of 5-par. fit)

- two reconstruction algorithms
- three pileup correction algorithms

FOM vs. E/E_{max} threshold for T/R, A, Q

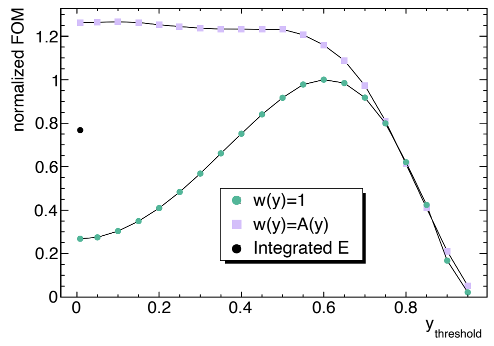

$R(\omega_a)$ Run 1 measurement inputs

Run 1a

R Run1a [ppb]	CA	EA	SA	WA	BT	CT	ET	ST	WT	BR	KQ
val	-28228.822	-28481.292	-28422.823	-28637.307	-28802.286	-28211.122	-28884.793	-28739.823	-28619.947	-28966.786	-29206.209
unc	1208.499	1201.164	1211.680	1221.856	1360.841	1338.227	1334.718	1335.002	1332.590	1361.011	2068.321
stat	1207.920	1193.750	1206.100	1218.350	1358.170	1337.677	1332.700	1331.350	1330.790	1359.810	2058.500
syst	37.401	133.251	116.155	92.493	85.226	38.373	73.370	98.683	69.237	57.160	201.322
Time randomization seed	6.536	26.020	27.000	16.000	20.200	6.711	31.370	22.500	16.000	22.500	0.000
Time correction	6.726	0.000	0.000	0.000	0.000	5.310	0.000	0.000	0.000	0.000	0.000
Cluster time assignment	0.000	1.000	1.000	1.000	1.000	0.000	1.000	1.000	1.000	1.000	0.000
In-fill gain amplitude	4.411	21.431	1.900	14.300	7.790	3.905	23.620	2.500	15.300	2.718	5.000
In-fill gain time constant	5.612	0.000	1.000	0.000	20.222	5.532	0.000	2.300	0.000	11.689	8.000
STDP gain amplitude	0.177	0.099	0.000	2.600	0.091	0.005	0.103	0.000	0.800	0.053	0.000
STDP gain time constant	0.734	0.000	0.000	0.000	0.000	0.145	0.000	0.000	0.000	0.000	0.000
Pileup covariance matrix	0.000	0.000	0.000	0.000	0.000	0.000	0.000	0.000	0.000	0.000	15.000
Pileup amplitude	0.744	16.211	14.000	13.800	21.700	0.905	17.245	19.800	16.200	19.900	0.000
Pileup cluster time model	0.000	58.921	47.000	0.000	5.100	0.000	12.502	8.500	0.000	6.400	0.000
Pileup cluster energy model	0.000	7.005	11.000	0.000	11.000	0.000	11.658	12.000	0.000	10.900	0.000
Pileup phase	0.000	0.000	0.000	39.600	0.000	0.000	0.000	0.000	5.500	0.000	0.000
Pileup time/energy bias	0.150	0.000	0.000	0.000	0.000	0.027	0.000	0.000	0.000	0.000	0.000
Pileup rate error	0.033	0.000	0.000	0.000	0.000	0.193	0.000	0.000	0.000	0.000	0.000
Unseen pileup	0.946	1.100	0.300	10.000	0.800	3.413	5.300	5.400	10.000	0.600	0.000
Triple pileup correction	0.000	4.600	4.400	1.000	1.900	0.000	3.300	4.200	1.000	1.600	0.000
Pileup simulation	0.000	0.000	0.000	0.000	0.000	0.000	0.000	0.000	0.000	0.000	10.000
Pileup artificial dead time	0.000	67.700	0.000	0.000	0.000	0.000	0.000	0.000	0.000	0.000	0.000
Loss covariance matrix	0.000	0.000	0.000	0.000	0.000	0.000	0.000	0.000	0.000	0.000	0.000
Loss time cuts	0.808	0.000	1.000	0.000	0.300	0.876	0.000	1.000	0.000	0.300	0.000
Loss energy cuts	0.000	0.000	0.500	0.000	0.500	0.000	0.000	0.500	0.000	0.300	0.000
Loss statistics	1.596	0.000	0.000	0.000	0.000	1.522	0.000	0.000	0.000	0.000	0.000
Loss detection efficiency	1.075	0.000	0.000	0.000	0.000	1.952	0.000	0.000	0.000	0.000	0.000
Fixed loss scale	0.000	0.000	0.000	0.000	0.000	0.000	0.000	0.000	0.000	0.900	0.000
Higher-order coincidences	0.000	0.700	0.500	0.000	0.000	0.000	0.700	0.500	0.000	0.000	17.000
CBO frequency change	5.638	11.600	7.100	19.000	10.900	4.299	9.800	5.600	17.000	5.300	5.500
CBO decoherence envelope	24.046	39.700	19.700	26.000	38.300	23.226	22.000	17.500	26.500	5.500	4.100
CBO time constants	4.145	14.200	2.000	11.000	10.800	8.079	2.700	2.000	13.000	10.800	6.000
Fixed CBO time constant	0.000	0.000	0.000	0.000	0.000	0.000	0.000	0.000	0.000	0.000	0.000
Vertical drift	0.000	0.000	0.000	0.000	0.000	0.000	0.000	0.000	0.000	0.000	198.000
Muon precession period	0.000	0.000	0.000	0.000	0.000	0.000	0.000	0.000	0.000	2.300	0.000
Muon lifetime	0.000	0.000	0.000	0.000	0.000	0.000	0.000	0.000	0.000	0.000	0.000
Ad hoc correction	5.593	5.000	77.700	27.000	28.700	0.445	12.000	78.000	4.000	22.900	0.000

Run 1b

R Run1b [ppb]	CA	EA	SA	WA	BT	CT	ET	ST	WT	BR	KQ
val	-26946.590	-27021.291	-27091.047	-26965.693	-27044.193	-27209.341	-27080.591	-27001.927	-27004.863	-27209.293	-24946.396
unc	1025.180	1018.880	1025.971	1035.843	1157.710	1135.268	1121.992	1129.788	1129.631	1158.484	1759.574
stat	1023.271	1012.020	1022.280	1030.180	1156.130	1133.584	1120.300	1128.100	1127.740	1157.420	1747.800
syst	62.548	118.034	86.946	108.166	60.455	61.811	61.587	61.745	65.338	49.651	203.212
Time randomization seed	5.484	23.600	17.100	13.000	19.100	5.663	26.300	19.500	14.000	20.100	0.000
Time correction	1.473	0.000	0.000	0.000	0.000	1.024	0.000	0.000	0.000	0.000	0.000
Cluster time assignment	0.000	1.000	1.000	1.000	1.000	0.000	1.000	1.000	1.000	1.000	0.000
In-fill gain amplitude	2.373	6.475	6.400	20.900	3.282	3.857	6.662	3.500	22.600	0.529	4.000
In-fill gain time constant	3.668	0.000	2.300	0.000	9.776	10.372	0.000	7.700	0.000	3.231	2.000
STDP gain amplitude	0.075	0.089	0.000	0.400	0.042	0.009	0.068	0.000	1.400	0.042	0.000
STDP gain time constant	0.443	0.000	0.000	0.000	0.000	0.343	0.000	0.000	0.000	0.000	0.000
Pileup covariance matrix	0.000	0.000	0.000	0.000	0.000	0.000	0.000	0.000	0.000	0.000	15.000
Pileup amplitude	0.489	14.033	12.000	12.500	11.400	0.818	6.644	10.600	7.000	11.400	0.000
Pileup cluster time model	0.000	64.159	53.000	0.000	4.600	0.000	14.223	7.200	0.000	4.800	0.000
Pileup cluster energy model	0.000	8.041	8.000	0.000	4.800	0.000	11.189	11.000	0.000	7.200	0.000
Pileup phase	0.000	0.000	0.000	42.500	0.000	0.000	0.000	0.000	6.000	0.000	0.000
Pileup time/energy bias	0.162	0.000	0.000	0.000	0.000	0.029	0.000	0.000	0.000	0.000	0.000
Pileup rate error	0.017	0.000	0.000	0.000	0.000	0.004	0.000	0.000	0.000	0.000	0.000
Unseen pileup	2.912	2.900	1.600	10.000	1.300	1.764	0.500	8.100	10.000	0.100	0.000
Triple pileup correction	0.000	4.959	4.800	1.000	1.300	0.000	1.476	2.900	1.000	1.200	0.000
Pileup simulation	0.000	0.000	0.000	0.000	0.000	0.000	0.000	0.000	0.000	0.000	10.000
Pileup artificial dead time	0.000	60.900	0.000	0.000	0.000	0.000	0.000	0.000	0.000	0.000	0.000
Loss covariance matrix	0.000	0.000	0.000	0.000	0.000	0.000	0.000	0.000	0.000	0.000	0.000
Loss time cuts	1.490	0.000	1.000	0.000	0.100	1.451	0.000	1.000	0.000	0.100	0.000
Loss energy cuts	0.000	0.000	0.500	0.000	0.100	0.000	0.000	0.500	0.000	0.100	0.000
Loss statistics	0.770	0.000	0.000	0.000	0.000	0.727	0.000	0.000	0.000	0.000	0.000
Loss detection efficiency	0.618	0.000	0.000	0.000	0.000	0.577	0.000	0.000	0.000	0.000	0.000
Fixed loss scale	0.000	0.000	0.000	0.000	0.000	0.000	0.000	0.000	0.000	3.400	0.000
Higher-order coincidences	0.000	0.600	0.500	0.000	0.000	0.000	1.100	0.500	0.000	0.000	3.000
CBO frequency change	14.216	12.200	12.500	18.000	22.500	12.135	11.200	11.800	15.000	0.700	16.000
CBO decoherence envelope	2.490	7.100	2.800	10.000	3.700	8.044	13.700	2.900	7.000	9.100	1.000
CBO time constants	41.888	2.600	11.000	45.000	23.100	36.225	3.500	9.000	30.000	21.800	8.000
Fixed CBO time constant	0.000	0.000	0.000	0.000	0.000	0.000	0.000	0.000	0.000	2.800	0.000
Vertical drift	0.000	0.000	0.000	0.000	0.000	0.000	0.000	0.000	0.000	0.000	200.000
Muon precession period	0.000	0.000	0.000	0.000	0.000	0.000	0.000	0.000	0.000	2.300	0.000
Muon lifetime	0.000	0.000	0.000	0.000	0.000	0.000	0.000	0.000	0.000	0.000	0.000
Ad hoc correction	19.560	17.000	13.800	37.300	11.800	19.470	33.000	34.000	14.700	15.300	0.000

Run 1c

R Run1c [ppb]	CA	EA	SA	WA	BT	CT	ET	ST	WT	BR	KQ
val	-27553.151	-27599.792	-27744.007	-27572.324	-27917.094	-28020.191	-27888.992	-27893.477	-27898.924	-27921.794	-26279.397
unc	824.775	820.274	825.993	834.914	932.719	912.906	909.385	909.687	909.909	934.158	1447.337
stat	823.995	814.609	822.380	830.450	930.105	912.601	906.720	908.410	907.900	932.710	1403.200
syst	35.871	96.237	77.167	86.224	69.778	23.610	69.568	48.189	60.439	51.987	354.703
Time randomization seed	4.512	18.300	13.300	10.000	16.000	4.647	18.900	14.700	11.000	18.100	0.000
Time correction	1.178	0.000	0.000	0.000	0.000	1.142	0.000	0.000	0.000	0.000	0.000
Cluster time assignment	0.000	1.000	1.000	1.000	1.000	0.000	1.000	1.000	1.000	1.000	0.000
In-fill gain amplitude	2.876	9.086	3.700	13.100	4.529	3.484	9.947	6.000	12.000	1.484	4.000
In-fill gain time constant	4.754	0.000	1.200	0.000	5.394	2.993	0.000	2.500	0.000	0.943	3.000
STDP gain amplitude	0.157	0.217	0.000	0.400	0.213	0.110	0.274	0.000	1.400	0.266	0.000
STDP gain time constant	0.727	0.000	0.000	0.000	0.000	0.570	0.000	0.000	0.000	0.000	0.000
Pileup covariance matrix	0.000	0.000	0.000	0.000	0.000	0.000	0.000	0.000	0.000	0.000	15.000
Pileup amplitude	0.370	9.751	8.000	10.000	8.100	0.557	5.263	8.000	6.000	10.100	0.000
Pileup cluster time model	0.000	57.190	44.000	0.000	5.500	0.000	12.330	6.700	0.000	5.600	0.000
Pileup cluster energy model	0.000	6.535	12.300	0.000	6.100	0.000	1.716	11.000	0.000	10.200	0.000
Pileup phase	0.000	0.000	0.000	38.300	0.000	0.000	0.000	0.000	5.300	0.000	0.000
Pileup time/energy bias	0.147	0.000	0.000	0.000	0.000	0.027	0.000	0.000	0.000	0.000	0.000
Pileup rate error	0.119	0.000	0.000	0.000	0.000	0.119	0.000	0.000	0.000	0.000	0.000
Unseen pileup	0.335	1.100	2.800	10.000	2.500	1.446	0.600	5.000	10.000	2.500	0.000
Triple pileup correction	0.000	3.900	3.600	1.000	1.000	0.000	1.360	2.300	1.000	1.100	0.000
Pileup simulation	0.000	0.000	0.000	0.000	0.000	0.000	0.000	0.000	0.000	0.000	10.000
Pileup artificial dead time	0.000	0.000	0.000	0.000	0.000	0.000	0.000	0.000	0.000	0.000	0.000
Loss covariance matrix	0.000	0.000	0.000	0.000	0.000	0.000	0.000	0.000	0.000	0.000	0.000
Loss time cuts	1.094	0.000	1.000	0.000	0.100	1.173	0.000	1.000	0.000	0.100	0.000
Loss energy cuts	0.000	0.000	0.500	0.000	0.100	0.000	0.000	0.500	0.000	0.100	0.000
Loss statistics	0.728	0.000	0.000	0.000	0.000	0.697	0.000	0.000	0.000	0.000	0.000
Loss detection efficiency	7.602	0.000	0.000	0.000	0.000	7.928	0.000	0.000	0.000	0.000	0.000
Fixed loss scale	0.000	0.000	0.000	0.000	0.000	0.000	0.000	0.000	0.000	3.100	0.000
Higher-order coincidences	0.000	0.700	0.500	0.000	0.000	0.000	0.800	0.500	0.000	0.000	2.000
CBO frequency change	12.971	17.300	13.100	21.000	21.300	11.399	15.000	11.600	18.000	1.600	48.400
CBO decoherence envelope	4.883	15.700	8.000	7.000	13.400	2.044	9.500	6.100	5.500	0.200	14.000
CBO time constants	7.536	15.900	6.000	9.000	23.400	4.965	35.500	12.000	25.000	30.900	28.000
Fixed CBO time constant	0.000	0.000	0.000	0.000	0.000	0.000	0.000	0.000	0.000	0.700	0.000
Vertical drift	0.000	0.000	0.000	0.000	0.000	0.000	0.000	0.000	0.000	0.000	342.000
Muon precession period	0.000	0.000	0.000	0.000	0.000	0.000	0.000	0.000	0.000	2.300	0.000
Muon lifetime	0.000	0.000	0.000	0.000	0.000	0.000	0.000	0.000	0.000	0.000	0.000
Ad hoc correction	21.403	17.000	4.000	47.600	24.400	6.620	18.000	7.600	22.400	19.100	0.000

Run 1d

R Run1d [ppb]	CA	EA	SA	WA	BT	CT	ET	ST	WT	BR	KQ
val	-27590.211	-27727.592	-27694.497	-27669.444	-27701.994	-27715.241	-27877.192	-27665.847	-27714.364	-27765.394	-27990.498
unc	677.405	672.330	677.201	682.522	761.733	748.292	744.367	747.218	744.932	759.068	1288.346
stat	675.823	667.947	672.860	679.850	758.400	747.400	743.493	744.140	743.690	757.600	1269.000
syst	46.264	76.641	76.558	60.337	71.176	36.532	36.069	67.757	42.992	47.187	222.428
Time randomization seed	3.632	12.600	11.900	6.000	12.300	3.737	10.900	11.000	7.000	13.700	0.000
Time correction	1.024	0.000	0.000	0.000	0.000	3.218	0.000	0.000	0.000	0.000	0.000
Cluster time assignment	0.000	1.000	1.000	1.000	1.000	0.000	1.000	1.000	1.000	1.000	0.000
In-fill gain amplitude	0.042	3.850	5.100	9.800	2.368	0.048	0.643	9.000	14.100	1.032	8.000
In-fill gain time constant	0.694	0.000	3.300	0.000	13.293	0.808	0.000	7.300	0.000	6.585	2.000
STDP gain amplitude	0.122	0.086	0.000	2.600	0.074	0.095	1.200	0.000	0.800	0.095	0.000
STDP gain time constant	0.594	0.000	0.000	0.000	0.000	0.504	0.000	0.000	0.000	0.000	0.000
Pileup covariance matrix	0.000	0.000	0.000	0.000	0.000	0.000	0.000	0.000	0.000	0.000	15.000
Pileup amplitude	0.355	8.809	7.000	6.300	10.100	0.348	10.378	5.600	9.500	9.400	0.000
Pileup cluster time model	0.000	47.500	41.000	0.000	5.000	0.000	7.527	5.600	0.000	4.800	0.000
Pileup cluster energy model	0.000	7.000	7.000	0.000	10.000	0.000	8.439	10.000	0.000	6.800	0.000
Pileup phase	0.000	0.000	0.000	34.900	0.000	0.000	0.000	0.000	4.400	0.000	0.000
Pileup time/energy bias	0.101	0.000	0.000	0.000	0.000	0.019	0.000	0.000	0.000	0.000	0.000
Pileup rate error	0.089	0.000	0.000	0.000	0.000	0.003	0.000	0.000	0.000	0.000	0.000
Unseen pileup	0.142	0.800	3.500	10.000	4.100	0.232	0.700	0.200	10.000	2.400	0.000
Triple pileup correction	0.000	4.637	3.900	1.000	1.600	0.000	2.330	1.400	1.000	1.300	0.000
Pileup simulation	0.000	0.000	0.000	0.000	0.000	0.000	0.000	0.000	0.000	0.000	10.000
Pileup artificial dead time	0.000	0.000	0.000	0.000	0.000	0.000	0.000	0.000	0.000	0.000	0.000
Loss covariance matrix	0.000	0.000	0.000	0.000	0.000	0.000	0.000	0.000	0.000	0.000	0.000
Loss time cuts	2.035	0.000	1.000	0.000	0.100	2.024	0.000	1.000	0.000	0.100	0.000
Loss energy cuts	0.000	0.000	0.500	0.000	0.100	0.000	0.000	1.000	0.000	0.500	0.000
Loss statistics	0.802	0.000	0.000	0.000	0.000	0.778	0.000	0.000	0.000	0.000	0.000
Loss detection efficiency	1.171	0.000	0.000	0.000	0.000	0.861	0.000	0.000	0.000	0.000	0.000
Fixed loss scale	0.000	0.000	0.000	0.000	0.000	0.000	0.000	0.000	0.000	0.100	0.000
Higher-order coincidences	0.000	0.400	0.500	0.000	0.000	0.000	1.200	0.500	0.000	0.000	3.000
CBO frequency change	0.634	25.000	13.300	23.000	22.200	0.606	1.400	0.500	21.000	8.500	33.000
CBO decoherence envelope	38.083	5.000	3.200	1.000	25.300	32.052	9.600	9.200	1.500	18.000	38.000
CBO time constants	7.053	0.600	1.000	2.000	10.500	3.316	0.800	8.000	6.000	9.800	3.000
Fixed CBO time constant	0.000	0.000	0.000	0.000	0.000	0.000	0.000	0.000	0.000	0.000	0.000
Vertical drift	0.000	0.000	0.000	0.000	0.000	0.000	0.000	0.000	0.000	0.000	208.000
Muon precession period	0.000	0.000	0.000	0.000	0.000	0.000	0.000	0.000	0.000	2.300	0.000
Muon lifetime	0.000	0.000	0.000	0.000	0.000	0.000	0.000	0.000	0.000	0.000	0.000
Ad hoc correction	3.544	6.000	38.000	7.000	18.800	0.518	13.200	58.000	12.000	6.700	0.000

11 ω_a measurement on each of 4 datasets

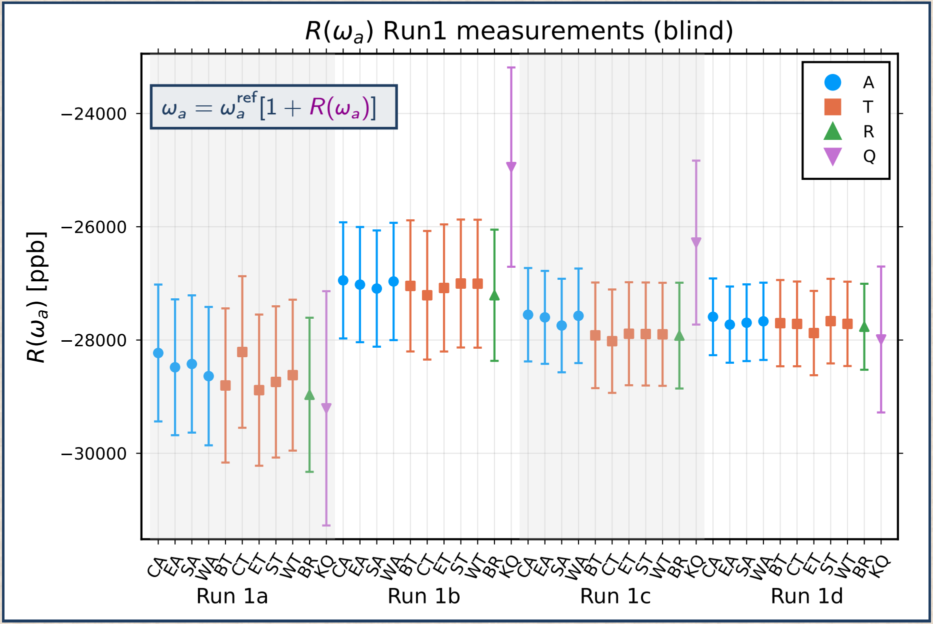

In each of 4 datasets, 11 ω_a measurements are consistent between each-other

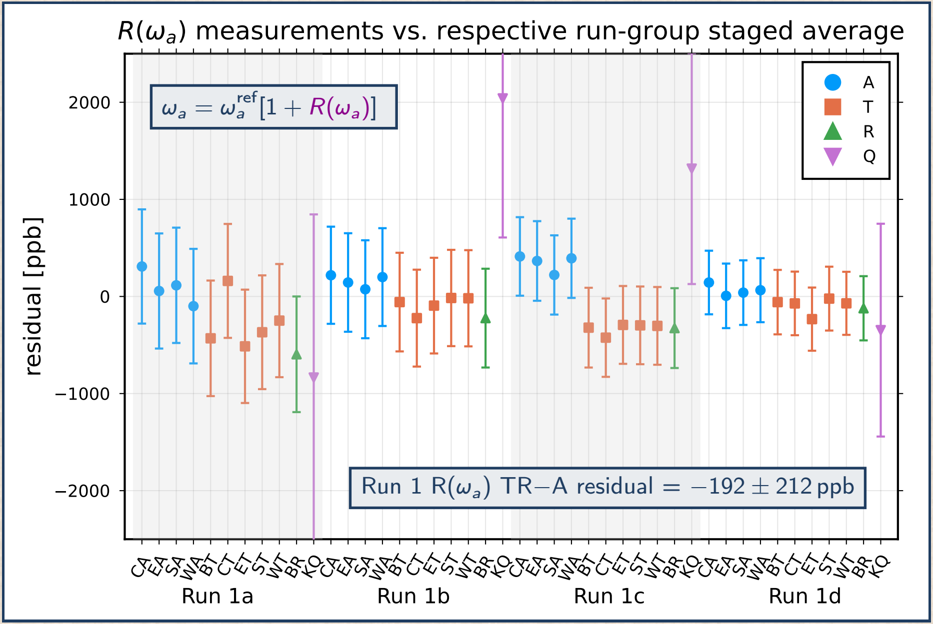

A large number of consistency checks has been completed

- fit results ought to be stable vs. chosen start time
- similar checks check performed vs.
  - calorimeter station
  - bunch number
  - Run number
  - time of day
  - positron energy bin
  - position within calorimeter
  - . . .

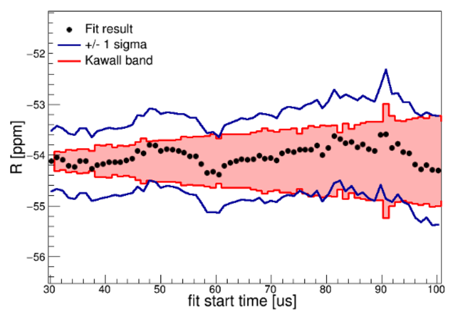

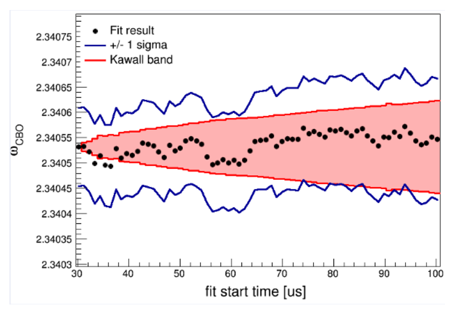

Average of 11 ~critically correlated measurements with imprecise correlation

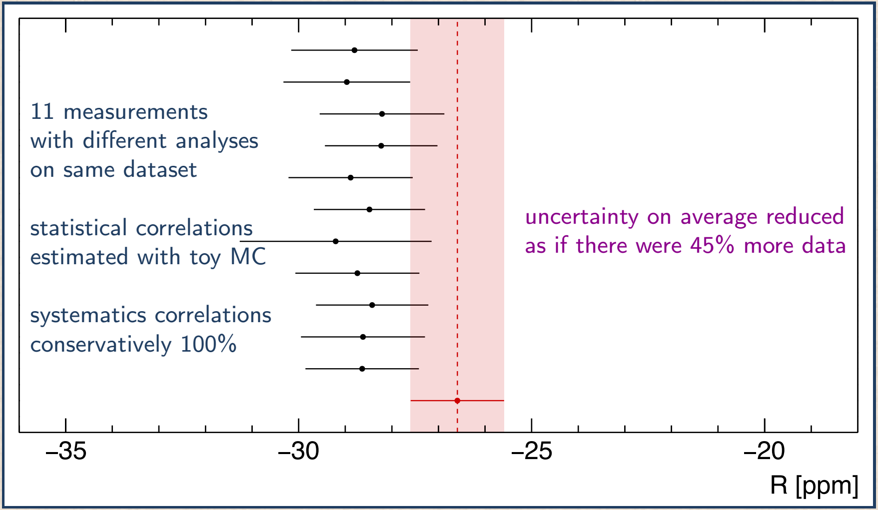

- statistical correlations estimations have limited precision
- systematic correlations estimated conservatively to avoid underestimation
- $\Rightarrow$ minimum χ^2 combination (=BLUE) not reliable

Critical correlation: $C_{ij}^{\text{crit}} = \rho^{\text{crit}} = \min(\sigma_i, \sigma_j)/\max(\sigma_i, \sigma_j) \quad (i \neq j)$

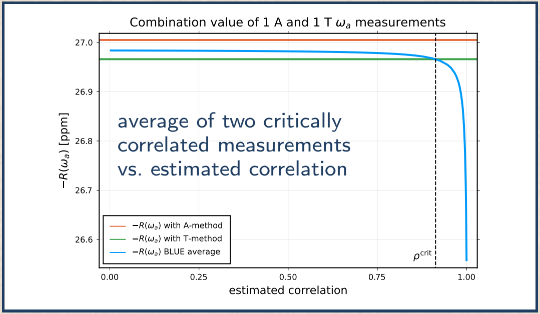

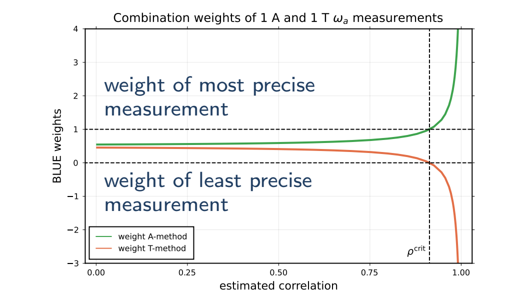

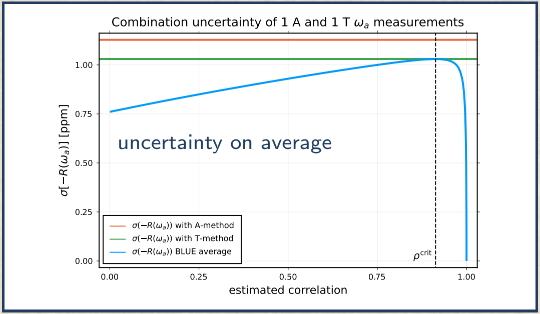

Least χ^2 average of 2 meas. around $\rho = \rho^{\text{crit}}$

- unstable vs. value of estimated correlation ρ
- Glen Cowan, Stat. Data Analysis, sec. 7.6.1
- Valassi & Chierici 2014, EPJC 74 (2014) 2017
- but no literature really appropriate for our case

Average the four most statistically precise A-method analyses
(on each of four datasets)

even weights, disregarding imprecise correlations

- 50% of weight to 1 A-method analysis using one of the two reconstructions
- 50% of weight to 3 A-method analyses using the other reconstruction
  - weight = 1/3 of 50% each
- robust procedure, close to optimal combination

measurements with methods T, R, Q used for checks

- T and R methods are ∼11% less precise than A (Q is even less precise)
- optimal combination T, R, Q weights non negligible only if T and/or R and/or Q measurements had much smaller systematics than A, which is not observed in present estimations

Synthetic ω_a^m FNAL Run 1 measurement

$R(\omega_a) = (\omega_a - \omega_a^{\mathrm{ref}}) \cdot 10^9$	FNAL Run 1 [ppb]	FNAL goal [ppb]	BNL [ppb]
value	-82357		
total uncertainty	437	122	487
statistical uncertainty	434	100	460
systematic uncertainty	56	70	160
- Gain changes	8	20	120
- Pileup	35	40	80
- Coherent Betatron Oscillation	38	30	70
- Time randomization (to remove "fast rotation")	9		
- Residual slow term	17		
- Other	3		

notes

- the FNAL total systematics goal includes other systematics that are not discussed here

Early to late effects

- unaccounted variations of conditions during muon fill time can induce biases on ω_a fit result

example of early-to-late effect: phase variation due to muon loss

- $N(t) = N_0 e^{-t/\tau_\mu} [1 + A\cos(\omega_a t + \varphi)]$ phase φ = muon spin-momentum angle at injection
- muon loss depends on momentum $\Rightarrow$ muon sample momentum varies $\bar{p} = \bar{p}(t)$
- single muon phase depends on momentum (because of production chain) $\bar{\varphi} = \bar{\varphi}(\bar{p})$
- at first order $$\bar{\varphi}(t) = \bar{\varphi}_0 + \frac{\mathrm{d}\bar{\varphi}}{\mathrm{d}t} t = \bar{\varphi}_0 + \frac{\mathrm{d}\bar{\varphi}}{\mathrm{d}\bar{p}}\frac{\mathrm{d}\bar{p}}{\mathrm{d}t} t \simeq \bar{\varphi}_0 + \bar{\varphi}' t$$
- muon rate modulation $\cos(\omega_a t + \bar{\varphi}(t)) \simeq \cos\left(\omega_a t + \bar{\varphi}_0 + \bar{\varphi}' t\right) = \cos[(\omega_a + \bar{\varphi}')t + \bar{\varphi}_0]$
  $\Rightarrow$ fit result for ω_a is biased when muon sample phase varies in the fit time window
- note: muon loss phase effect is different and additional to muon loss effect on positron rate

other early to late effects

- variation of calorimeter gain (corrected before the wiggle plot fit)
- variation of pileup (proportional to $[N(t)]^2$, corrected before the wiggle plot fit)
- variation of beam average position and size (phase acceptance)
- variation of magnetic field due to electric quadrupoles plates vibration
- variation of magnetic field due to kicker eddy currents

Electric field correction $C_e = +489 \pm 53\,\text{ppb}$

- compute momentum distribution from electrons detected at early times after injection
  - using cosine Fourier transform of rate vs. time
  - measuring change of shape of rectangular bunches (debunching)
- compute radial muon distribution from momentum distribution
- compute electric field contribution to ω_a due to quadrupoles electric field

cosine Fourier vs. debunching method

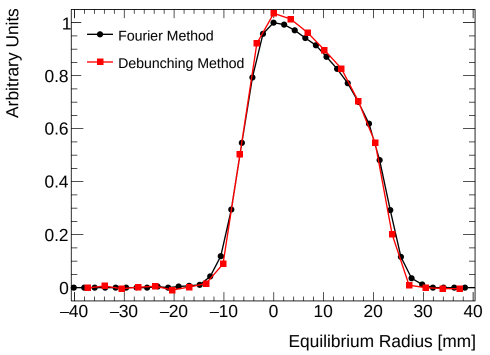

radial distributions in the four datasets

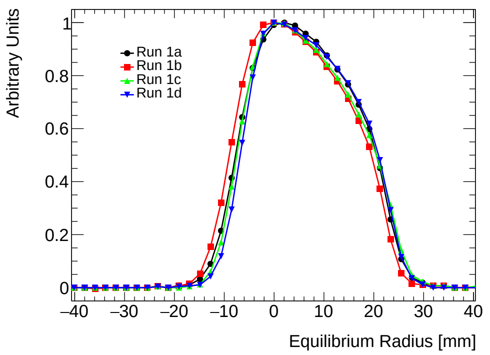

Pitch correction $C_p = +180 \pm 13\,\mathrm{ppb}$

- reconstruct muon vertical position from decay electrons measurend on trackers
- compute corresponding pitch correction to ω_a

vertical decay vertices distribution

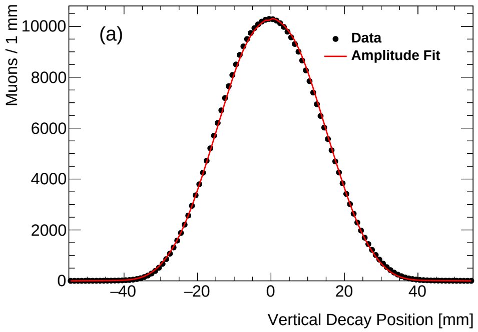

vertical oscittation amplitude distribution

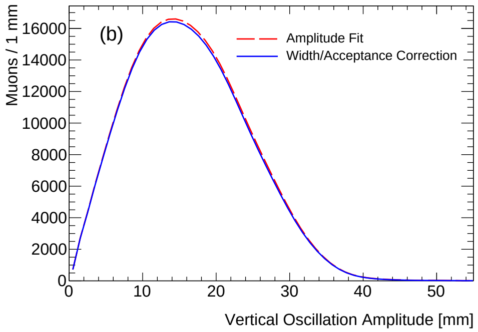

Lost muons phase-variation effect correction $C_{\mathrm{ml}} = -11 \pm 5\,\mathrm{ppb}$

measured and simulated $\varphi - p$ correlation

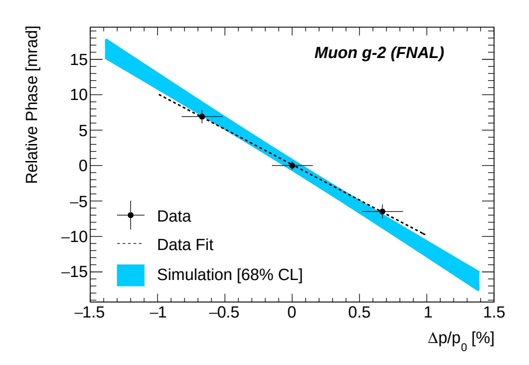

- $\mathrm{d}\varphi/\mathrm{d}p$ measured on dedicated runs by varying magnetic field by -0.68%, +0.68%
- measurement consistent with simulation

estimated $\Delta\varphi(t)$ due to muon loss

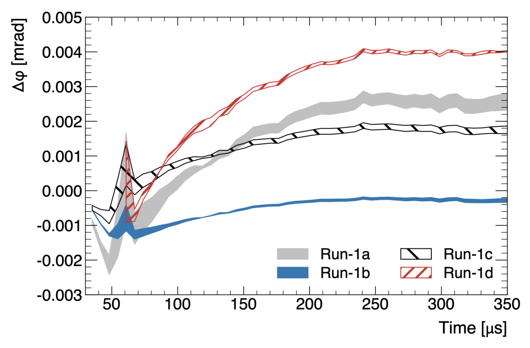

- use delivery ring collimators to change the muon momentum distribution
- muon loss function of time and momentum fitted using simulation-inspired analytic function to model observed beam loss for different muon momentum distributions

Phase-Acceptance correction $C_{pa} = -158 \pm 75$ ppb

- effective phase variation due to variation of beam horizontal and vertical position and spread
- example: $\Delta\omega_a = \frac{d\varphi}{dt} = \frac{d\varphi}{dY_{RMS}} \cdot \frac{dY_{RMS}}{dt}$
- obtained with simulation
- measured with trackers and extrapolated to whole ring with beam dynamics simulations

phase as a function of muon position

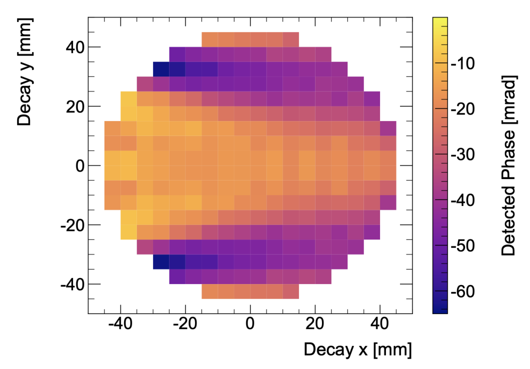

variation of Y_{RMS}

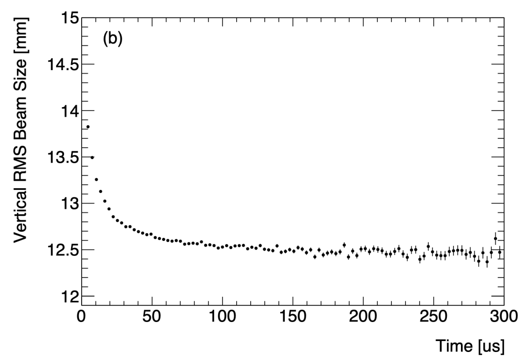

Measuring ω_p / magnetic field with fixed and trolley probes

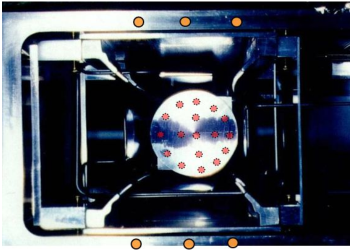

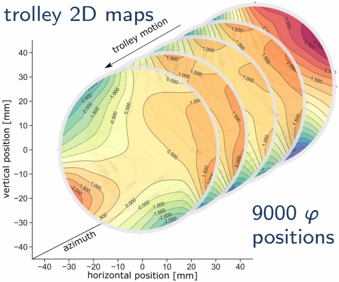

- 378 fixed probes measure continuosly the magnetic field
- 17-probes trolley run along muons path every ∼3 days
- fixed probes measurements corrected using trolley measurements

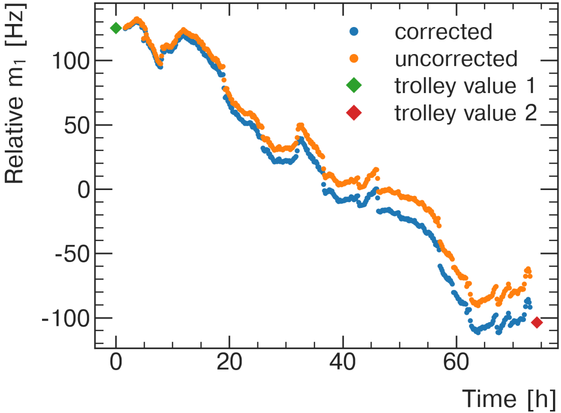

Measuring ω_p magnetic field: calibration of probes

calibration

- each trolley probe calibrated with absolute cylindrical probe placed in the same position inside the storage ring
- absolute cylindrical probe calibrated to reference absolute spherical probe in MRI magnet at Argonne National Laboratory
- absolute spherical probe consistent with novel absolute ^{3}He probe
- 17 probes calibration uncertainty 20 – 48 ppb

reference temperature

- magnetic field measurements corrected to be expressed as $\omega'_p(T)$, precession frequency of shielded proton spin in spherical water sample at reference temperature of 34.7 °C

absolute spherical probe

$\tilde{\omega}'_p(T)$ (magnetic field experienced by the muons) measured to 56 ppb

- tracker reconstructs muons decay vertices in parts of storage region
- bean dynamics simulation used to extrapolate to whole storage region
- magnetic field map averaged over muon distribution
- two independent groups did the measurement, one additional group the calibration

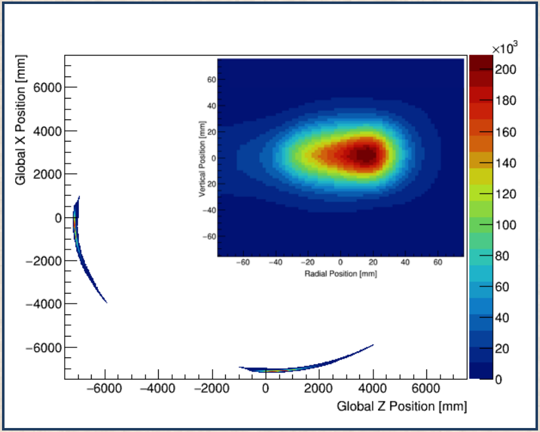

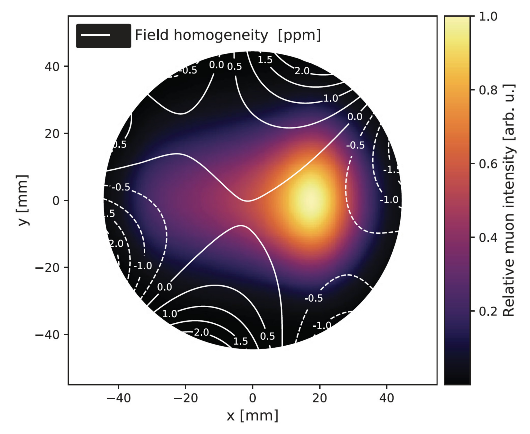

Electric quadrupoles transient field correction $B_q = -17 \pm 92$ ppb

- electric quadrupoles are pulsed (to prevent static charge accumulation)
- plates vibration perturbs magnetic field
- special NMR probes measure the transient field perturbation in muon region
- large uncertainty because mapping incomplete will improve in Run 2+

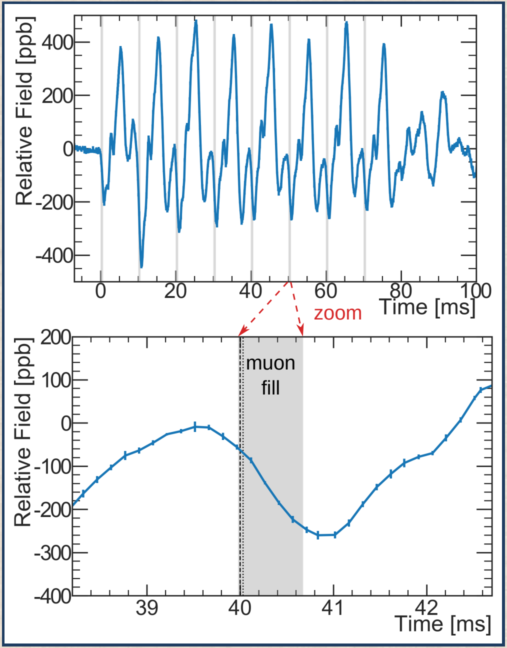

Kicker magnets transient field correction $B_k = -27 \pm 37$ ppb

- kicker magnets pulsed before start of fit window
- induced eddy currents perturb magnetic field inside fit window
- magnetic field perturbation measured with a Faraday effect magnetometer

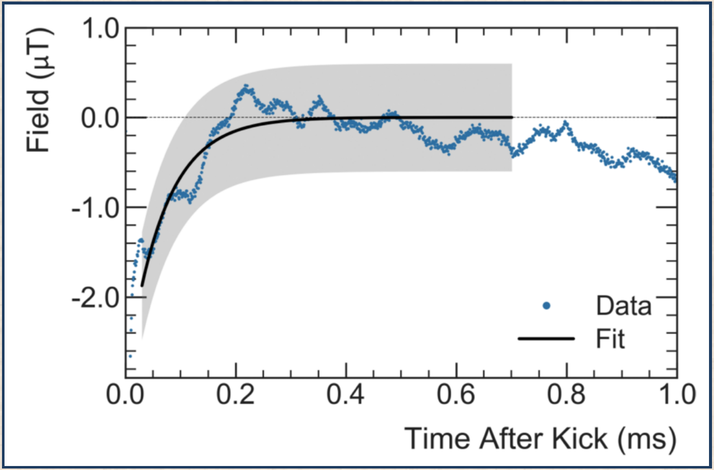

All corrections and uncertainties estimated before unblinding

	Correction	Uncertainty	Design goal
ω_a^m (statistical)	–	434	100
ω_a^m (systematic)	–	56	
base clock	–	2	
C_e	489	53	
C_p	180	13	
C_{ml}	-11	5	
C_{pa}	-158	75	
ω_a beam dynamics corrections $(C_e + C_p + C_{ml} + C_{pa})$	499	93	
ω_a total systematic	499	109	70
$\omega'_p(T)(x, y, \varphi)$	–	54	
$M(x, y, \varphi)$	–	17	
$\langle\omega'_p(T)(x, y, \varphi) \times M(x, y, \varphi)\rangle$	–	56	
B_q	-17	92	
B_k	-27	37	
$\tilde{\omega}'_p(T)$ transient fields corrections $(B_q + B_k)$	-44	99	
$\tilde{\omega}'_p(T)$ total [note: correction sign now for $\omega_a/\tilde{\omega}'_p(T)$]	44	114	70
$\omega_a/\tilde{\omega}'_p(T)$ total systematic	544	157	100
external measurements	–	25	
total [correction is for $\omega_a/\tilde{\omega}'_p(T)$]	544	462	140

Check consistency of $R'(T) = \omega_a/\tilde{\omega}'_p(T)$ for the four Run 1 datasets

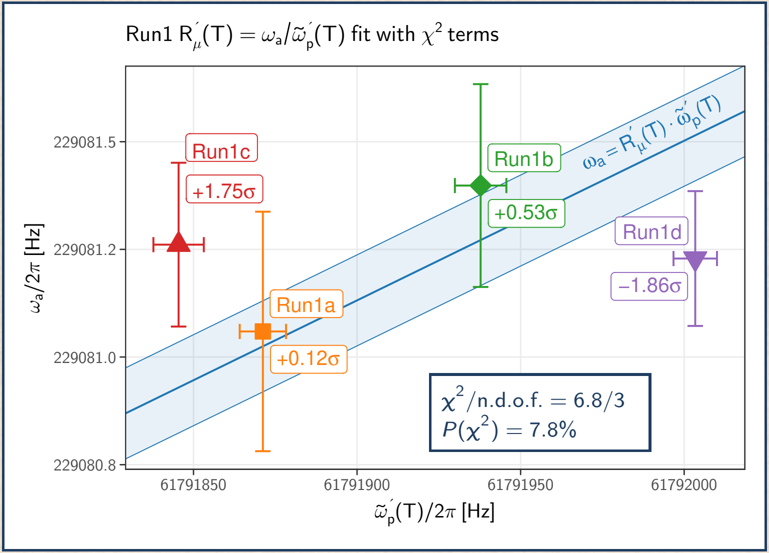

- reported χ^2 terms are larger than one can guess on the plot because uncertainties are partly correlated

Unanimous consensus for unblinding in a remote collaboration meeting

UW envelope

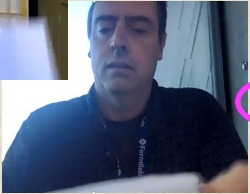

FNAL envelope

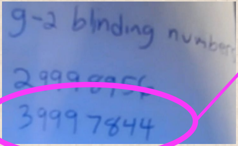

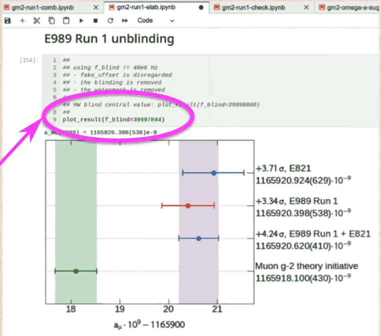

First FNAL Muon $g-2$ result

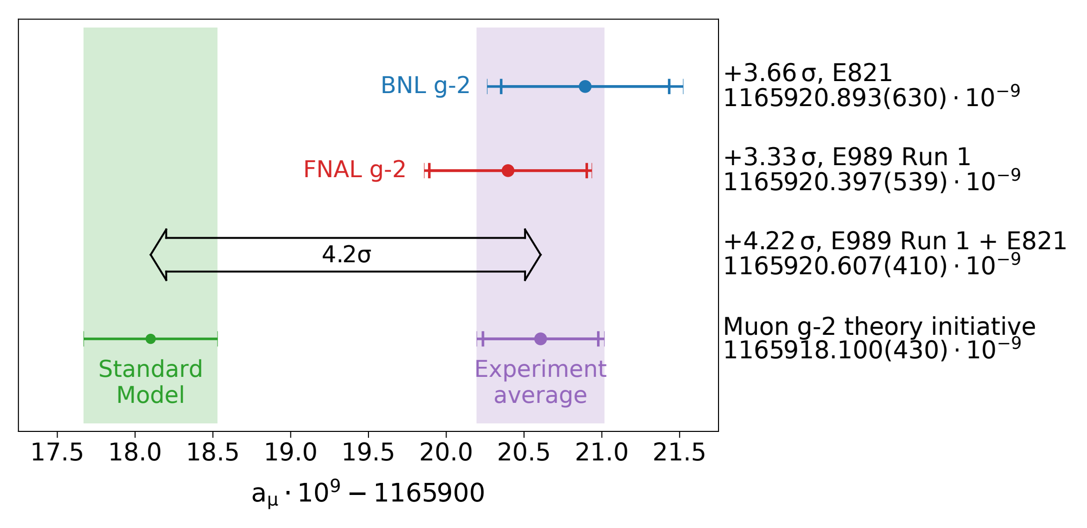

- a_μ(BNL) recomputed from R_μ(BNL) like a_μ(FNAL)
- included correlation due to external measurements, assumed no other correlation between BNL and FNAL

Three papers published on April 7, 2021, a fourth one accepted

- Measurement of the Positive Muon Anomalous Magnetic Moment to 0.46 ppm
  doi:10.1103/PhysRevLett.126.141801
- Measurement of the anomalous precession frequency of the muon in the Fermilab Muon $g-2$ Experiment
  doi:10.1103/PhysRevD.103.072002
- Magnetic Field Measurement and Analysis for the Muon $g-2$ Experiment at Fermilab
  doi:10.1103/PhysRevA.103.042208
- Beam dynamics corrections to the Run-1 measurement of the muon anomalous magnetic moment at Fermilab
  doi:10.1103/PhysRevAccelBeams.24.044002

New lattice QCD a_μ prediction (BMW 2021) published on 7 April 2021

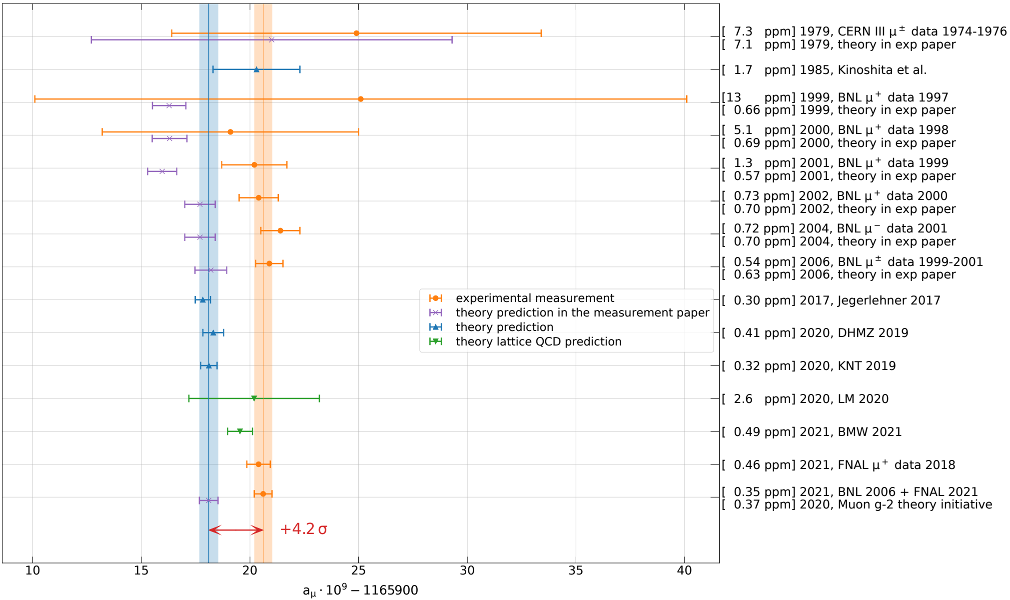

What comes next

FNAL-E989 experiment

- Run 1 is 6% of design goal sample
- measurement using Run 2+3 data in ∼1 year

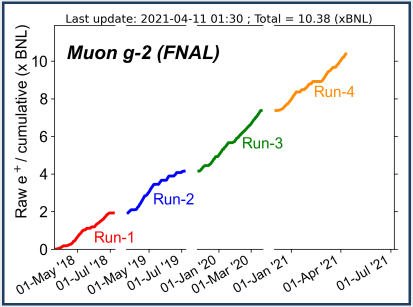

J-PARC Muon g-2/EDM experiment

- data-taking planned to start in 2024

Muon $g-2$ theory initiative

- review BMW 2021 lattice QCD prediction
- new $\sigma(e^+e^- \to \text{hadrons})$ measurements coming

New Physics models

- a_μ measurement provides improved constraints on New Physics modes and an improved experimental reference for selecting how NP models rank in fitting all observations

MuonE experiment

- measures t-channel $\mu - e$ scattering to compute HVP a_μ contribution

Muon g-2/EDM experiment at J-PARC

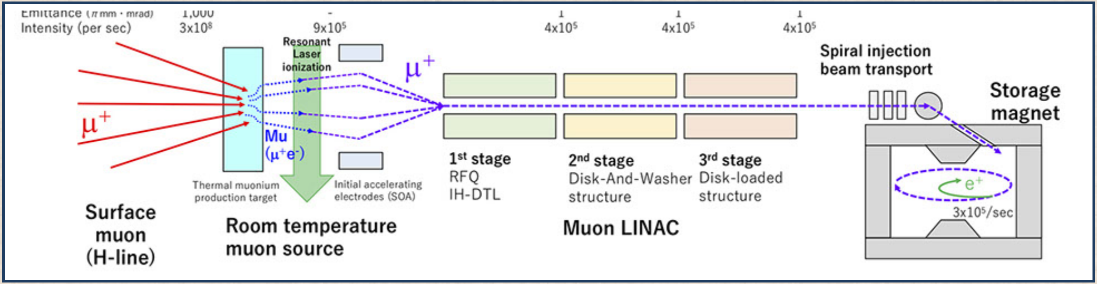

- 50% polarized 300 MeV muons
- small 3.0 T magnet
- no electric field, low focusing magnetic field
- silicon tracker instead of calorimetry
- $5.7 \cdot 10^{11}$ reconstructed electrons
- 0.45 ppm statistical uncertainty goal

Thanks for your attention!

Trasparenze addizionali

a_μ Standard Model test more powerful than a_e for high energy New Physics

a_μ test $\sim$2000$\times$ less precise than a_e test for experimental and theory uncertainties

$$\frac{\Delta(a_\mu^{\text{exp}} - a_\mu^{\text{th}})}{\Delta(a_e^{\text{exp}} - a_e^{\text{th}})} \sim 2000$$

but

a_μ test $\sim$43000$\times$ more sensitive than a_e test for "typical" high-energy New Physics models

$$\frac{a_\mu^{\text{New Physics}}}{a_e^{\text{New Physics}}} \sim \frac{m_\mu^2}{m_e^2} \simeq 43000$$

experiment and theory uncertainties contributions to a_μ test as of March 2021

	δa_μ [ppm]	δa_e [ppb]
experiment	0.54	0.24
theory	0.37	0.20
- α_{QED}	0.00	0.20
- QED	0.00	0.01
- EW	0.01	0.00
- QCD	0.37	0.01
- HVP	0.34	
- HLbL	0.15	

- note: using less precise α_{QED}(Cs 2018) because of inconsistency with α_{QED}(Rb 2020)

Main ω_a measurement systematics mentioned in E989 TDR

	E821 [ppb]	E989 improvement plans	goal [ppb]	Run 1 [ppb]
gain changes	120	better laser calibration low-energy threshold	20	20
pileup	80	low-energy samples recorded calorimeter segmentation	40	35
lost muons	90	better collimation in ring	20	5
CBO	70	higher n value (frequency) better match of beamline to ring	$<$30	38
E and pitch	50	improved tracker precise storage ring simulation	30	55
total	180		70	109

Beam dynamics frequencies

			f [MHz]	T [μs]
Anomalous precession	f_a		0.2291	4.3649
Cyclotron	f_c		6.7024	0.1492
Horizontal betatron	f_x	$= f_c\sqrt{1-n}$	6.2874	0.1590
Vertical betatron	f_y	$= f_c \cdot \sqrt{n}$	2.3218	0.4307
Coherent betatron oscillation	f_{CBO}	$= f_c - 1 \cdot f x$	0.4150	2.4097
Vertical oscillation	f_{VO}	$= f_c - 1 \cdot f y$	4.3806	0.2283
Vertical waist	f_{VW}	$= f_c - 2 \cdot f y$	2.0589	0.4857

field index $n = 0.12$